



Sedimentology of a 'non-actualistic' Middle Ordovician tidal-influenced reservoir in the Murzuq Basin (Libya)

Marc Gil-Ortiz, Neil David McDougall, Patricia Cabello, Mariano Marzo, and Emilio Ramos

AAPG Bulletin published online March 1, 2019
doi: 10.1306/02151918138

Disclaimer: The AAPG Bulletin Ahead of Print program provides readers with the earliest possible access to articles that have been peer-reviewed and accepted for publication. These articles have not been copyedited and are posted "as is," and do not reflect AAPG editorial changes. Once the accepted manuscript appears in the Ahead of Print area, it will be prepared for print and online publication, which includes copyediting, typesetting, proofreading, and author review. ***This process will likely lead to differences between the accepted manuscript and the final, printed version.*** Manuscripts will remain in the Ahead of Print area until the final, typeset articles are printed. Supplemental material intended, and accepted, for publication is not posted until publication of the final, typeset article.

Cite as: Gil-Ortiz, M., N. D. McDougall, P. Cabello, M. Marzo, and E. Ramos, Sedimentology of a 'non-actualistic' Middle Ordovician tidal-influenced reservoir in the Murzuq Basin (Libya), (*in press; preliminary version published online Ahead of Print* March 1, 2019): AAPG Bulletin, doi: 10.1306/02151918138.

1 **Sedimentology of a ‘non-actualistic’ Middle Ordovician**
2 **tidal-influenced reservoir in the Murzuq Basin (Libya)**

3
4 Marc Gil-Ortiz^{1,3}, Neil David McDougall¹, Patricia Cabello^{2,3}, Mariano Marzo^{2,3}
5 and Emilio Ramos^{2,3}

6
7 ¹Repsol Exploración S.A. c/Méndez Álvaro, 44, 28045 (Madrid, Spain)

8 ²Departament de Dinàmica de la Terra i de l'Oceà. Facultat de Ciències de la
9 Terra. Universitat de Barcelona, c/Martí i Franquès s/n, 08028 (Barcelona,
10 Spain)

11 ³Institut de Recerca Geomodels. Universitat de Barcelona, c/Martí i Franquès
12 s/n, 08028 (Barcelona, Spain)

13
14 **ACKNOWLEDGMENTS**

15 Special thanks are due to the Libyan NOC, notably Bashir Garea and Khaeri
16 Tawengi, partners Total, Equinor and OMV both for the technical support in this
17 project and permission to publish the results. Special thanks are also due to
18 Edward Jarvis of CGG-Robertson for discussions concerning the key core
19 descriptions. Thanks are also to my colleagues Manuel Ron, Javier Buitrago,
20 Mikel Erquiaga, Lamin Amh Abushaala and Mourad Bellik for introducing me to
21 the project and their continuous help throughout the study. Special thanks to
22 Eduard Remacha and Francisco Pángaro for constructive discussions in the
23 field and in the office. Support from the Ministerio de Economía y
24 Competitividad (Project Sedimentary Sediment Routing Systems: Stratigraphic
25 Analysis and Models CGL2014-55900-P) and Generalitat de Catalunya

1 (2014SGR467) is gratefully acknowledged. Thanks to reviewers David Boote
2 and Jonathan Redfern and also to the editors of the AAPG Bulletin for their
3 constructive comments which have improved the content of this paper.

4

5 **ABSTRACT**

6 The subsurface of the highly productive Murzuq Basin in southwest Libya
7 remains poorly understood. As a consequence there is a need for detailed
8 sedimentological studies of both the oil-prone Mamuniyat Formation and Hawaz
9 Formation reservoirs in this area. Of particular interest in this case, is the Middle
10 Ordovician Hawaz Formation, interpreted as an excellent example of a 'non-
11 actualistic', tidally influenced clastic reservoir which appears to extend hundreds
12 of kilometers across much of the North African or Saharan craton. The Hawaz
13 Formation comprises 15 characteristic lithofacies grouped into 7 correlatable
14 facies associations, distributed in broad and laterally extensive facies belts
15 deposited in a shallow marine, intertidal to subtidal environment. Three main
16 depositional sequences and their respective systems tracts have also been
17 identified. On this basis a genetic-based stratigraphic zonation scheme has
18 been proposed as a tool to improve subsurface management of this reservoir
19 unit. A 'non-actualistic' sedimentary model is proposed in this work with new
20 ideas presented for marginal to shallow marine depositional environments
21 during the Middle Ordovician in the northern margin of Gondwana.

22

23 **Keywords:** Hawaz Formation, 'non-actualism', shallow marine, marginal
24 marine, ichnofacies

25

1 INTRODUCTION

2 For many years, the main Libyan petroleum province was the prolific Sirte Basin
3 with a limited contribution from the Ghadames Basin (Berkine Basin in Algeria)
4 (Hallet, 2002; Figure 1). However, since the mid-1990s, the Murzuq Basin has
5 developed into a major oil and gas producing province. The Hawaz Formation
6 constitutes one of the most important reservoirs in a number of producing fields
7 in the central and northern part of the basin. The generally high reservoir quality
8 (average 5-15% porosity and 0.1-150md permeability) and lateral continuity,
9 characteristic of the Hawaz are key factors in the development and production
10 of these accumulations. However, despite the well-documented potential of the
11 Hawaz Formation, its subsurface character remains poorly understood.

12 To date, only a few sedimentological studies of this formation have been carried
13 out and all are exclusively based on surface geology (Vos, 1981; Anfray and
14 Rubino, 2003; Marzo and Ramos, 2003, personal communication; Ramos et al.,
15 2006; Gibert et al., 2011). Other published works have focused on diagenesis
16 (Abouessa and Morad, 2009; Abouessa, 2012) and trapping mechanisms
17 (Franco et al., 2012). In addition, subsurface interpretations of the formation are
18 based on inconsistent lithostratigraphic correlations unconstrained by a
19 consistent sequence stratigraphic framework. As such there is no genetic or
20 sequence stratigraphy-based zonation. This limited database highlights the
21 necessity of providing a sequence stratigraphic framework based on a robust
22 sedimentological model of the transitional to shallow marine Hawaz Formation.

23 As Dalrymple and Choi (2007) have highlighted, transitional tide-dominated and
24 deltaic facies reflect the interaction of numerous terrestrial and marine
25 processes in a very complex depositional environment. Any paleoenvironmental

1 or stratigraphic interpretation of such transition zone successions requires a
2 comprehensive understanding of the facies and facies associations. Hence, a
3 comprehensive understanding of the facies changes through this transition zone
4 is necessary in order to make proper paleoenvironmental and sequence-
5 stratigraphic interpretations of the sedimentary successions. However, is it
6 actually possible to compare these paleoenvironments with any 'actualistic'
7 sedimentary model?

8 The limitations of the approach become apparent when the uniformitarian
9 principle is extended to depositional environments in the most ancient
10 geological record. In particular, the assumption that modern environments can
11 provide analogues for all geological successions must be questioned (Nichols,
12 2017). It is broadly accepted that earth dynamics have changed considerably
13 throughout geological history and accordingly, factors controlling sedimentation
14 have changed also, such as a lack of flora stabilizing river banks, greenhouse
15 vs icehouse periods defining coastal geomorphology, tidal ranges controlling
16 facies belts or characteristic ichnofacies during a particular period of geological
17 time. The analysis of some of these factors suggests that the facies succession
18 of the Hawaz Formation reflects rather different depositional processes from
19 those observed in modern environments. From this point forward we will use the
20 term 'non-actualistic' to describe those processes affecting the geological
21 signature of the Hawaz Formation which are difficult to compare with any
22 modern depositional environment analogue.

23 Consequently, the main aim of this article is to present a sedimentological
24 characterization of the Hawaz Formation based on a detailed lithofacies
25 description and interpretation together with the development of a facies

1 association classification. This forms the basis for an appropriate depositional
2 model in accordance with plausible physical and chemical processes during the
3 Middle Ordovician. In addition the overall analysis aims to build a genetically-
4 based zonation through sequence stratigraphy which will improve reservoir
5 management and provide tools for maximizing hydrocarbon recovery efficiency.
6 Finally, it is intended that these sedimentological and stratigraphic models
7 should be a well-documented subsurface analogue for clastic reservoirs in
8 similar settings.

9

10 **GEOLOGICAL SETTING**

11 *The structure and stratigraphy of the Murzuq Basin*

12 The Paleozoic succession of the Murzuq Basin is an erosional remnant of a
13 much more extensive regional succession extending along the northern margin
14 of the Gondwana supercontinent (Davidson et al., 2000; Shalbak, 2015). Its
15 present extent reflects several periods of uplift and unroofing during the late
16 Paleozoic, Mesozoic and Cenozoic, which together are responsible for its
17 modern architecture. As a consequence, the present-day basin geometry bears
18 little relation to the broader and larger pre-existing sedimentary basin. The
19 current basin is composed of a central Cretaceous depression bounded to the
20 northwest by the Atshan arch, the Gargaf high to the north, and the Tibesti and
21 Tihemboka highs on the southeast and southwest, respectively (Figure 1).
22 These structural highs were formed by multiphase tectonic uplifts from the
23 middle Paleozoic to Cenozoic, although the main periods of uplift and erosion
24 occurred during the Pennsylvanian (late Carboniferous; Hercynian) and early
25 Cenozoic (Alpine) orogenic cycles.

1 A series of geological events can be recognized in the stratigraphic record of
2 the Murzuq Basin, some represented by basin-scale unconformities within the
3 sedimentary infill reflecting the Pan-African, Caledonian and Hercynian
4 orogenesis and the short Late Ordovician glacial event responsible for the
5 Taconic or basal glacial erosional surface (Figure 2). Other unconformities that
6 may be recognized within the sedimentary record are minor or belong to the
7 younger Austrian or Alpine cycles, and consequently, they do not strongly affect
8 the Paleozoic section directly in the central Murzuq Basin; although, they may
9 have had strong implications in terms of overburden removal, source rock
10 maturity and reservoir quality due to uplift and unroofing of Mesozoic series on
11 the Paleozoic section (Boote et al., 2012).

12 The maximum sedimentary thickness in the present-day Murzuq Basin is about
13 4000 m (13,000 ft). Despite successive erosive episodes during several phases
14 of uplift throughout the history of the basin, the maximum sedimentary thickness
15 most probably never exceeded 5000 m (16,400 ft) (Davidson et al., 2000). The
16 age of the infill ranges from Cambrian to Cretaceous, often covered by large
17 Quaternary sand dunes in the central part of the basin. The sedimentary infill
18 can be subdivided into four main units: 1) Cambrian–Ordovician, 2) Silurian, 3)
19 Devonian–Carboniferous, and 4) Mesozoic (Figure 2).

20 The lower Paleozoic succession comprises the terrigenous Cambrian–
21 Ordovician Gargaf Group consisting of at least five formations – from bottom to
22 top: Hasawnah, Ash Shabiyat, Hawaz, Melaz Shuqran and Mamuniyat
23 Formations (Figure 2). The lowermost Hasawnah Formation rests
24 unconformably on the Precambrian basement and is composed of Cambrian to
25 Lower Ordovician conglomeratic to sandy continental and shallow marine littoral

1 deposits. The Hasawnah Formation is overlain, above a transgressive surface
2 of erosion, by the shallow marine and preglacial Ash Shabiyat and Hawaz
3 Formations, attributed respectively to the Lower and Middle Ordovician
4 (Tremadocian-Sandbian). The Upper Ordovician succession, associated with a
5 major glaciation, principally comprises the Melaz Shuqran and Mamuniyat
6 Formations, locally overlain by a thin and somewhat enigmatic package known
7 as the Bir Tlacin. The former is most probably lower Hirnantian and
8 predominantly mud-prone representing the period of the highest relative sea
9 level during the Late Ordovician (McDougall and Martin, 2000) whereas the
10 Mamuniyat Formation is a major Hirnantian sand-prone package.

11

12 *The petroleum systems and the hydrocarbon production history of the Murzuq*
13 *Basin*

14 Early exploration in the Murzuq Basin focused upon surface structures. The first
15 exploratory well was drilled in the northern Murzuq in 1955-56. Subsequently, a
16 number of successful discoveries in the neighbouring Illizi Basin (southeastern
17 Algeria) encouraged further exploration across the border. Three years later
18 Exxon discovered gas at Atshan region and Gulf tested oil at low rates from
19 Ordovician sandstones. However, in 1958, industry attention shifted east with
20 the discovery of a major oil accumulation in the Sirte Rift province and there
21 was little further exploration of the Murzuq Basin for the next 20 years. During
22 the late 1980s to 1990s, Rompetrol and later Repsol drilled up to 57 exploratory
23 wells in the basin, all of which targeted Ordovician prospects. This exploratory
24 activity resulted in many significant oil discoveries highlighting the rapidly
25 growing potential of the basin.

1 The most recent hydrocarbons-in-place estimation for the Murzuq Basin is
2 about 6 billion barrels (bbl) of oil and about 35 trillion cubic feet (TCF) of gas,
3 which represent about 6.5% of the Libya's resources and 30% of the Libya's
4 current oil production (Shalbak, 2015).

5 The main petroleum system in the Murzuq Basin comprises a basal Silurian
6 (Tanezzuft) hot-shale source rock, Ordovician sandstone reservoirs and a thick
7 Tanezzuft shale seal (Figure 2). A secondary petroleum system in the basin
8 (noncommercial to date) is composed of the basal Devonian sandstones (BDS)
9 as reservoirs and the intra-Devonian shales as the seal (Hallet, 2002; Shalbak,
10 2015), which also involves the basal Silurian hot-shale source rock (Fello et al,
11 2006; Hall et al, 2012).

12 The Ordovician sandstone reservoirs, associated with the primary petroleum
13 system, are the Middle Ordovician Hawaz Formation and the Upper Ordovician
14 Mamuniyat Formation, separated by a deeply incised unconformity related to
15 the Late Ordovician glaciation. This succession was cut by north-northwest to
16 west-flowing Hirnantian glaciers (Ghienne et al., 2003; Le Heron et al., 2004)
17 eroding down into the Hawaz Formation to create a rugged landscape of
18 paleovalleys and highs ('buried hills'). The valleys were partially infilled by the
19 periglacial to subglacial Melaz Shuqran, Mamuniyat and Bir Tlacsin clastics and
20 the residual topography subsequently buried by Tanezzuft shales. This
21 sometimes sealed the Hawaz erosional highs to form paleotopographic traps
22 with now reservoir significant volume of hydrocarbons (Figure 2).

23

24 *The Hawaz Formation*

1 In the subsurface of the northern Murzuq Basin, the Hawaz Formation is
2 represented by a detrital succession of slightly more than 200 m (650 ft) thick,
3 composed of fine-grained quartz arenites and subarkosic arenites, with
4 subordinate sublithic arenites, similar to the equivalent succession exposed on
5 the Gargaf High (Ramos et al., 2006).

6 Trace fossils are frequent and, locally, abundant enough to overprint most
7 primary sedimentary structures (Ramos et al., 2006). Gibert et al. (2011),
8 identify eleven ichnogenera, which exhibit a close relationship with both
9 lithofacies and depositional paleoenvironments (facies associations). In broad
10 terms, nearshore to shoreface facies are dominated by dense 'pipe rock' fabric
11 formed by *Skolithos* and *Siphonichnus*. In contrast, storm-dominated heterolithic
12 facies are characterized by horizontal deposit feeding *Cruziana* bioturbation.

13 Two main paleocurrent trends have been identified by Ramos et al. (2006): a)
14 small-scale sedimentary structures including ripples and small sigmoidal cross-
15 bedded sets, indicative of widely dispersed flow directions and b) large scale
16 sedimentary structures suggesting a dominant flow towards the northeast and
17 northwest but locally with bidirectional currents.

18 A number of sedimentary models have been proposed for the Hawaz
19 Formation, but all within transitional to shallow marine setting. Vos (1981)
20 suggested the outcrop succession represented a fan-delta complex. Other
21 authors (i.e. Anfray and Rubino, 2003; Ramos et al., 2006) identified
22 sedimentary structures indicative of strong tidal influence and the latter
23 proposed a tide-dominated model with deposition in a mega-estuary or gulf
24 where the morphology of the paleocoastline enhanced tidal action, especially
25 during transgressive episodes, when the coastal embayment was flooded.

1 Measured porosity can reach up to 25.7% although values around 15 to 16%
2 are the most frequent. Pore connectivity is good with pore throat diameters
3 ranging from 0.1 μm to 64 μm (average 14.6 μm). Measured horizontal
4 permeability values from core plugs may reach 900 to 1000 md (Shalbak, 2015)
5 although most commonly average values in wells are around 0.2 to 150md. On
6 the other hand, diagenetic alterations have also had an impact on reservoir
7 quality as noted by Abouessa and Morad (2009). Specifically, the presence of
8 higher amounts of feldspar, illite, a higher dickite to kaolinite ratio and more
9 abundant quartz cement, compared with those sampled in outcrops, is possibly
10 due to the longer residence time under deep burial conditions.

11

12 **DATABASE AND METHODOLOGY**

13 The present study was based on data from 36 wells located across the north
14 central sector of the Murzuq Basin (Figure 3). This data included core
15 descriptions, high-resolution image logs (FMI), gamma-ray (GR), sonic (DT),
16 neutron porosity (NPHI) and density (RHOZ) wireline logs. The methodology
17 followed consisted of:

18 1) Well data synthesis and standardization from the 36 wells by means of
19 building well composite charts with the wireline logs available for each well.

20 2) Description and interpretation of the sedimentary facies based on 14 cored
21 wells and FMI data. Conventional wireline logs were not used to define
22 lithofacies at this stage as the typical thickness of most lithofacies units is
23 below the vertical resolution of these tools. The resultant facies analysis was
24 compared with previous outcrop descriptions from the northern Gargaf high
25 by Marzo and Ramos (2003, personal communication), Ramos et al. (2006)

1 and Gibert et al. (2011) and used as an analogue for subsurface
2 correlations.

3 3) Grouping the resultant lithofacies into facies associations, defined by cores
4 and FMI logs, each with distinct wireline log profiles and stacking patterns.
5 These log profiles were then used to identify facies associations in wells
6 lacking core or FMI data.

7 4) Construction of a comprehensive depositional model defined by the
8 lithofacies and facies associations identified in cores, FMI logs and
9 conventional wireline log profiles.

10 5) Sequence stratigraphic analysis of the Hawaz Formation. Vertical changes
11 in facies associations and their stacking patterns were used to identify
12 correlatable stratigraphic genetic units. These units were then preliminary
13 traced throughout the study area and used to define the sedimentary
14 architecture of the Hawaz succession (Gil-Ortiz et al. personal
15 communication).

17 **SEDIMENTOLOGY OF THE HAWAZ FORMATION**

18 **Lithofacies**

19 Fifteen Hawaz lithofacies were defined in the subsurface of the central Murzuq
20 Basin based upon their lithology and internal fabric including sedimentary
21 structures and bioturbation (Table 1). These include sandstones (S), muddy
22 sandstones (MS), heterolithic sandstones (HS) and heterolithic mudstones
23 (HM). These lithofacies have been compared with those outcropping in the
24 Gargaf high as described by Marzo and Ramos (2003, personal
25 communication) and Ramos et al. (2006), and complemented with valuable

1 ichnofacies observations from outcrops described by Gibert et al. (2011). Each
2 of the lithofacies is described and interpreted as follows:

3 *Large scale cross-bedded sandstones (Sx1)*

4 Fine-grained, well-sorted and cross-bedded sandstones with high-angle
5 foresets ($>15^\circ$) (Figure 4) characterized by a N-NW directed paleoflow derived
6 from image log dip picking. Locally, mud drapes and rare mudstone intraclasts
7 line set bases and foresets. There is no evidence of bioturbation. Typically,
8 these sandstones form sets more than 50 cm (20 in) thick and cosets up to 10
9 m (33 ft) thick. The cross bedding is interpreted as a response to the migration
10 of dune bedforms under conditions of net sedimentation. The mud-draped
11 foresets reflect alternating periods of slack water in a tidal regime. The lack of
12 detrital clays and bioturbation suggests moderate to high energy conditions,
13 under which the fines were carried off in suspension. Equivalent lithofacies have
14 been described by Ramos et al. (2006) in outcrops as large-scale, sigmoidal
15 cross-bedded sandstones with occasional horizontal trace fossils (*Cruziana*
16 ichnofacies).

17 *Small to medium scale cross-bedded sandstones (Sx2)*

18 Fine to medium-grained, well-sorted and cross-bedded sandstones
19 characterized by low-angle (5° to 15°) foresets (Figure 4) again characterized by
20 a N-NW directed paleoflow as suggested by image log interpretation. Planar
21 lamination, current ripple cross lamination, mud drapes, and mudstone
22 intraclasts also occur locally. The degree of bioturbation ranges from absent to
23 weak with rare *Planolites*. It forms sets up to 50 cm (20 in) thick. The cross
24 stratification and cross lamination record the migration of medium-scale dunes

1 and ripples and megaripples, respectively, under the influence of unidirectional
2 current flow. This lithofacies could also be interpreted as corresponding to
3 toesets of the previous described large-scale cross-bedded sandstones (i.e.
4 lithofacies Sx1). Most probably deposition occurred within a high energy tidally
5 influenced environment. Equivalent lithofacies have been described by Ramos
6 et al. (2006) outcropping as medium-scale, sigmoidal cross-bedded sandstones
7 with occasional horizontal trace fossils (*Cruziana* ichnofacies).

8 *Parallel-laminated sandstones (Sl)*

9 Fine-grained sandstones with parallel lamination ($<5^\circ$) (Figure 4). Bioturbation
10 was not recognized (Figure 4). Organized in sets 10 to 100 cm (4 to 39 in) thick.
11 It is interpreted to record sand deposition from nearshore currents under a
12 moderate to high-energy, upper flow regime. A similar lithofacies has been
13 described by Ramos et al. (2006) in outcrops as parallel-laminated sandstones
14 with occasional parting lineation and very scarce bioturbation.

15 *Cross-laminated sandstones (Sxl)*

16 Fine-grained sandstones with low-angle cross-lamination (Figure 4). Climbing-
17 ripple lamination and mud drapes are also occasionally present. In general, it is
18 a nonbioturbated lithofacies, although sparse *Skolithos* were occasionally
19 observed. Set thicknesses range from 10 to 140 cm (4 to 55 in). This lithofacies
20 is interpreted as the deposits of storm events in a nearshore environment.
21 When climbing ripples are present, a high rate of sedimentation under
22 unidirectional flows is inferred. Similar lithofacies are described by Ramos et al.
23 (2006) outcropping in the Gargaf high as low-angle, swaley (SCS) to hummocky
24 cross-stratified sandstones (HCS).

1 *Ripple cross-laminated sandstones (Sr)*

2 Fine-grained very well sorted sandstones with ripple cross-lamination and
3 locally intraclasts. Occasionally the current ripples display bimodal foreset
4 directions. Bedset or coset thickness does not exceed 50 cm (20 in) whilst
5 individual sets are up to 3 cm (~1 in) thick typically associated with very thin
6 clay drapes (Figure 4). This is an unbioturbated lithofacies. The cross-
7 lamination records the migration of current ripples under low to moderate
8 velocity currents. The presence of clay drapes and the bimodal foreset
9 directions, observed in some sets, would suggest deposition in a subtidal
10 setting. Equivalent ripple cross-laminated sandstones with occasional horizontal
11 trace fossils (*Cruziana* ichnofacies) have also been identified in outcrop by
12 Ramos et al. (2006) characterized by a dominantly north-northwest paleoflow
13 direction, locally bimodal towards south-southeast.

14 *Massive sandstones (Sv)*

15 Fine-grained, clean, generally well sorted sandstones with poorly defined planar
16 lamination and cross-bedding (Figure 4). Locally, mud intraclasts and basal
17 erosive surfaces were identified. This lithofacies is characterized by the
18 absence of bioturbation. It is organized forming sets of 30 to 100 cm (10 to 39
19 in) thick. The massive appearance of this facies could be interpreted as the
20 result of early postdepositional processes involving dewatering and partial
21 fluidization suggestive of a high sedimentation rate in the depositional system.
22 This lithofacies can be easily misinterpreted as Sx1 in cores when the clean
23 nature of the sandstones, reflecting the lack of micas and fine sediment
24 obscures the limits between cross-bed sets. The lack of detrital clays and micas

1 in these sandstones suggests deposition in a relatively high-energy
2 environment where fines were carried off in suspension. Equivalent lithofacies
3 have been observed by Ramos et al. (2006) outcropping in the northern margin
4 of the basin as apparently massive sandstones.

5 *Burrowed cross-bedded sandstones (Sxb)*

6 Clean, fine-grained sandstones displaying small to medium-scale cross bedding
7 with local mudstone intraclasts. Moderate degree of bioturbation with *Skolithos*
8 and *Siphonichnus* burrows (Figure 4). Typically organized in 30 to 200 cm (10
9 to 79 in) thick beds. The clean nature of the sandstones and the presence of
10 mudstone intraclasts suggest moderate to high energy conditions in which fines
11 were carried off in suspension. The cross-bedding records the migration of dune
12 and bar bedforms whereas the vertical to oblique burrows suggest a shallow,
13 high energy marine environment.

14 *Burrowed cross-laminated sandstones (Sxlb)*

15 Fine-grained, variably argillaceous and micaceous sandstones with low-angle
16 cross-lamination and local mud laminae and mudstone intraclasts. This
17 lithofacies is moderately bioturbated with an ichnofabric dominated by *Skolithos*
18 and *Siphonichnus*, indeterminate burrows and meniscate backfilled burrows
19 (Figure 4). The minimum thickness observed of this lithofacies is 70 cm (28 in).

20 The moderately intense bioturbation, dominated by mainly vertical, suspension-
21 feeding burrows suggests a shallow, high-energy subtidal environment.
22 However, the mud laminae also reflect low-energy conditions. Thus, depending
23 on the context, this lithofacies may have different interpretations ranging from a
24 lower shoreface to an intertidal environment. The low-angle cross-lamination is

1 interpreted as reflecting deposition from subtidal sand sheets or low relief sand
2 bars.

3 *Burrowed ripple cross-laminated sandstones (Srb)*

4 Very fine- to fine-grained sandstones, locally argillaceous and micaceous
5 characterized by current-ripple cross-lamination and planar lamination. A
6 moderate degree of bioturbation characterizes this lithofacies (Figure 4), with an
7 ichnofabric dominated by *Skolithos* (6 – 8 mm [0.24 – 0.31 in] diameter and
8 maximum length of 30 cm [12 in]), *Siphonichnus* and local indeterminate
9 burrows. This lithofacies forms packages 15 to 170 cm (6 to 67 in) thick. The
10 fine grain size and the locally argillaceous composition of this lithofacies imply
11 deposition in a relatively low energy environment. The cross-lamination records
12 the migration of current ripples under conditions of net sedimentation and
13 implies that the sand was transported by a unidirectional current of low to
14 moderate velocity. The ichnofauna (mostly represented by vertical burrows)
15 suggests a shallow marine environment dominated by suspension feeding
16 benthonic fauna.

17 *Burrowed sandstones with Siphonichnus (Sb)*

18 Fine-grained well-sorted sandstones locally with mud laminae. This lithofacies is
19 highly bioturbated, with an ichnofauna dominated by *Siphonichnus* burrows,
20 locally up to 100 cm (39 in) in length, giving rise to a distinctive 'pipe rock'
21 fabric. The minimum bed thickness appears to be about 20 cm (8 in), although
22 bed boundaries are typically obscured by bioturbation (Figure 4); This
23 lithofacies is volumetrically very abundant and continuous sections of up to 20
24 m (66 ft) have been identified in some wells. The occurrence of vertical burrows

1 (*Skolithos* ichnofacies) suggests a moderate- to low-energy, restricted to
2 shallow-marine environment, and the presence of mud laminae (mud drapes)
3 implies fluctuating energy levels. Equivalent lithofacies have been described by
4 Ramos et al. (2006) in outcrops as thick-bedded, massive, bioturbated
5 sandstones.

6 *Burrowed sandstones with feeding ichnofauna (MSb)*

7 Argillaceous fine-grained sandstones characterized by moderately intense
8 bioturbation dominated by horizontal, deposit feeding burrows (Figure 4);
9 notably *Teichichnus* and *Thalassinoides*. Individual beds range in thickness
10 from 10 to 270 cm (4 to 106 in). The moderately high detrital clay content of
11 these sandstones and the characteristic low-energy ichnofauna suggests a
12 relatively protected depositional setting or open-marine conditions.

13 *Sandy heterolithic (HS)*

14 Interbedded very fine- to fine-grained sandstones and argillaceous siltstones
15 (>50% sand content). This lithofacies displays flaser structures together with
16 combined current and wave ripple cross-lamination and also planar lamination
17 (Figure 4). There is only a limited amount of bioturbation with rare *Chondrites*
18 and *Planolites* burrows. The thickness of this lithofacies ranges between 1 cm
19 (0.4 in) sets up to an accumulated bedset thickness of 5 m (16 ft). The
20 interbedding of sandstone and argillaceous siltstone implies fluctuating energy
21 levels. Sands were transported and deposited by both unidirectional and
22 oscillatory (wave-generated) flows. Unidirectional current flow was mostly of low
23 to moderate velocity, resulting in the formation of current ripples. By contrast,
24 the presence of cross-bedding (due to the migration of dune and bar bedforms)

1 and mudstone intraclasts indicates higher current velocities. The presence of
2 *Chondrites* indicates that burrowing took place under marine conditions; the
3 remaining burrows, *Planolites* and indeterminate horizontal tubes, also suggest
4 a marine environment. The low bioturbation index together with the local
5 occurrence of *Chondrites* (generally considered to be characteristic of low
6 oxygen conditions), suggests that oxygenation levels were low. Wave, current
7 and combined-flow cross-lamination suggests sands were deposited during
8 storm events below fair-weather wave base.

9 *Burrowed sandy heterolithics (HSb)*

10 Thinly interbedded very fine-grained, micaceous, argillaceous sandstone and
11 micaceous, argillaceous siltstone (>50% sand content). Locally, the argillaceous
12 siltstones display planar lamination and the sandstones current and wave ripple
13 cross lamination. Bioturbation is moderately intense characterized by
14 overprinted *Skolithos* and *Cruziana* ichnofacies (*Siphonichnus* burrows, with
15 subordinate *Planolites* and indeterminate burrows) (Figure 4). Minimum bed
16 thickness is 1 cm (0.4 in) whereas accumulated bedset thickness can reach 4 m
17 (13 ft). The interbedding of sandstone and siltstone suggests fluctuating energy
18 conditions, with the sandstones representing higher energy levels. The cross
19 lamination within the sandstones records the migration of combined current and
20 wave ripples under conditions of net sedimentation and low to moderate current
21 velocities. The mixed assemblage of ichnofauna suggests the transition from a
22 high-energy to a low-energy setting, from an open-marine inner shelf up to a
23 lower shoreface setting. There is a variation of this lithofacies in the upper part
24 of the Hawaz Formation, where the base of the sandy intervals occasionally
25 displays rip-up mudstone clasts and a rhythmic alternation of thin, inclined, mud

1 drapes and sandstones. In this case, the interpretation given to this lithofacies
2 corresponds to inclined heterolithic stratification (IHS) associated with minor
3 channels or tidal creeks in a restricted, sandy to mixed intertidal
4 subenvironment.

5 *Muddy heterolithics (HM)*

6 Mudstones interbedded with micaceous argillaceous siltstone and very fine-
7 grained sandstone (>50% clay content). The mudstone and argillaceous
8 siltstone display planar lamination and lenticular bedding (current and wave
9 rippled sand lenses). The sandstone contains current ripples and rare wave
10 ripples (Figure 4). Individual lithofacies packages have a minimum thickness of
11 5 cm (2 in) but may reach an accumulated bedset thickness up to 3.5 m (11.5
12 ft). The sandstone beds and lenses represent energetic pulses in an overall low
13 energy setting, where mud settled out of suspension. During the higher-energy
14 pulses, sand was moved by both unidirectional and oscillatory (wave-
15 generated) flows. The lack of burrows indicates anoxic conditions in a fairly
16 distal marine setting or a restricted and stressed subenvironment, such as a
17 tidal mudflat or lagoon.

18 *Burrowed muddy heterolithics (HMb)*

19 Argillaceous siltstone interbedded with minor fine-grained sandstone layers and
20 sandstone laminae (>50% clay content). It is characterized by a variable degree
21 of bioturbation with *Siphonichnus*, *Skolithos*, *Planolites* and indeterminate
22 vertical burrows (Figure 4). Shrinkage cracks may occur locally. The minimum
23 thickness of individual facies units is 7 cm (3 in) whilst the accumulated bedset
24 thickness is up to 3.8 m (12.5 ft). The interbedding of argillaceous siltstone and

1 very fine- to fine-grained sandstone suggests fluctuating energy conditions in an
2 overall low-energy setting. The shrinkage cracks are probably related to
3 variations in salinity and temperature when present. The depositional setting of
4 this lithofacies varies from a relatively distal, inner shelf subenvironment to a
5 restricted intertidal flat subenvironment.

6 **Facies associations**

7 The proposed scheme based on the previously described lithofacies establishes
8 7 facies associations designated as HWFA1 to HWFA7 assigned to proximal
9 and increasingly distal environments (Figure 5).

10 HWFA1: Tidal flat

11 Facies association HWFA1 mainly consists of lithofacies Sxlb, MSb, Sb, HMb
12 and HSb with subordinate Srb and Sv (Figure 5). The thickness of individual
13 packages of this facies association is very variable, ranging from 30 to 60 m
14 (100 to 200 ft), as a direct consequence of the downcutting associated with the
15 Upper Ordovician glaciogenic unconformities. The GR log response varies
16 significantly from 30 to 140 API units in a characteristic fining-upward
17 succession . The intensity of bioturbation is moderate to very high;
18 characterized by a mixed low diversity *Skolithos* and *Cruziana* ichnofacies
19 assemblage indicative of a relatively high-energy environment grading towards
20 a more protected and restricted low-energy setting. It is also characterized by
21 an upwards-increasing detrital clay content typical of tidal flat environments.
22 Furthermore, the low diversity of acritarch assemblages and the strong
23 predominance of leiospheres, characteristic of a marginal-marine setting,
24 identified in palynological studies of some wells, suggests a relatively protected

1 tidal sand to mixed flat environment grading normally from the underlying
2 HWFA3 or HWFA2 (see below). Some ichnogenera identified as *Planolites*,
3 *Siphonichnus* and *Thalassinoides* strongly associated with tidal flat deposits
4 (Gingras et al., 2012) also support this hypothesis, together with the common
5 occurrence of clay drapes and flaser-lenticular bedding (Figure 6-A). The
6 sporadic occurrences of individual massive to rippled sandstones levels (Sv and
7 Srb) and the presence of rip-up mudstone clasts at the base of these units in
8 the heterolithic intervals (locally associated with small synsedimentary faults)
9 are interpreted in terms of bank collapse in tidal creeks on the sand flat. The
10 same package in the Gargaf high was described as an upper shoreface wave
11 dominated facies assemblage by Ramos et al. (2006) which probably would
12 represent a beach to barrier island setting laterally equivalent to this facies
13 association HWFA1.

14 *HWFA2: Subtidal complex*

15 Facies association HWFA2 is mainly composed of lithofacies Sx2, Sx1, Sxl, Sr,
16 Sl and Sv with subordinate HM (Figure 5). It is organized into stacked packages
17 0.3 to 40 m (1 to 131 ft) thick. The basal contact of these packages is typically
18 erosive, locally marked by the presence of mud clasts (Figure 6-B) and the GR
19 response is both clean and blocky (GR values around 25 API units) locally
20 marked by peaks (up to 65 API units) related to the presence of thin mud-
21 drapes or concentrations of mica . These values are within the established
22 range for micaceous sandstones which could have values of up to 80 API units
23 (Rider, 2004). Bioturbation is scarce to absent, probably related to a very high
24 sediment supply in a relatively short period of time. Paleocurrents, measured in
25 this facies association from image log data, indicate a dominant trend towards

1 the north-northwest with some bidirectionality, probably related to tidal effects
2 as indicated by the mud drapes in lithofacies Sx1, Sx2 and Sr (Figure 6-C).
3 However, an additional secondary trend has also been identified indicating flow
4 toward the northeast. The reservoir quality of this facies association is the best
5 of the entire Hawaz Formation with an average porosity of 11% and an average
6 horizontal permeability of 125md.

7 Facies association HWFA2 is interpreted as an amalgamated complex of sand
8 bars and dunes (slightly coarsening-upwards profile with Sx1, Sx2 and Sr
9 lithofacies), and channel deposits (slightly fining-upwards profile with Sv, Sl
10 and Sr lithofacies) influenced by the action of the tides. The interpretation is a
11 laterally extensive fluvio-tidal to subtidal complex. Subordinate heterolithic
12 intervals are also found intercalated with the cross-stratified sand bars, possibly
13 related to periods of slack water and deposition in relatively protected lagoonal
14 or interbar subenvironments. The features of this facies association are very
15 similar to those described by Ramos et al. (2006) from the Gargaf high 100 km
16 (62 mi) to the north. They are almost equivalent in depositional environment
17 although in the subsurface of the northern Murzuq Basin HWFA2 would
18 represent a shallower lateral equivalent with higher fluvial influence due to the
19 general absence of bioturbation reflecting higher energy and sedimentation
20 rates.

21

22 *HWFA3: Abandoned subtidal complex*

23 Facies association HWFA3 is primarily characterized by lithofacies Sx1b, Sxb,
24 Srb, Sxl, Sv and Sx2 (Figure 5). It forms packages ranging in thickness from 0.6
25 to 12 m (2 to 40 ft). Facies packages are distinguished by a fining-upward

1 succession of fine-grained sandstones represented by a distinctive upwards
2 increase in the GR characterized by API values between 25 and 70.
3 Bioturbation is moderate typically becoming more abundant towards the upper
4 part of these successions with common *Skolithos* and *Siphonichnus* burrows.

5 This facies association is interpreted to represent the abandonment of the
6 associated subtidal complex (HWFA2) after a general rise in relative sea level
7 and a cessation or major decrease in sediment supply promoting colonization in
8 a subtidal setting. It is quite common to find this facies association gradationally
9 intercalated with the subtidal complex reflecting a transgressional trend in a
10 relatively protected environment.

12 *HWFA4: Middle to lower shoreface*

13 Facies association HWFA4 is mainly composed of lithofacies Sr, Srb, Sxlb, Sxb,
14 Sv, HSb (Figure 5). The thickness of individual packages ranges between 0.6
15 and 14 m (2 and 46 ft). The GR response is typically a serrate, coarsening-
16 upwards succession with values ranging between 30 and 80 API units (Figure
17 9). Bioturbation varies from scarce to moderate. Overall packages of this facies
18 association form clear coarsening-upwards successions with a characteristic
19 *Skolithos* ichnofacies related to regressive sand belts prograding during
20 highstand sea-level conditions (Gibert et al., 2011). On this basis, the
21 interpretation proposed is of a low to moderate-energy, middle to lower
22 shoreface setting prograding in a relatively high-energy subtidal environment.

23 *HWFA5: Burrowed shelfal and lower shoreface*

1 Facies association HWFA 5 mainly consists of lithofacies Sb, MSb and Sxlb
2 (Figure 5). Thickness of individual packages ranges between 0.6 and 33 m (2
3 and 108 ft). The typical GR log response of this facies association is irregularly
4 serrate with values between 30 and 80 API units , reflecting a relative increase
5 in the detrital clay content. Bioturbation is moderate to very abundant tending to
6 overprint and obscure all primary sedimentary structures (Figure 6-D).

7 This facies association is interpreted to have been deposited in a lower
8 shoreface to shelf environment as suggested by the variably clean to
9 argillaceous nature of the sandstones and ubiquitous bioturbation with a well-
10 developed *Skolithos* ichnofacies.

11 12 *HWFA6: Burrowed inner shelf*

13 Facies association HWFA6 comprises lithofacies HMb and HSb (Figure 5). The
14 minimum thickness of individual packages is around 30 cm (1 ft) whilst the
15 maximum value is 15.8 m (52 ft). It may be considered as the distal equivalent
16 of HWFA5 characterized by a spiky GR response characterized by notably
17 higher values ranging from 60 to 120 API units . Bioturbation intensity is
18 moderate, with an ichnofaunal assemblage dominated by the *Cruziana*
19 ichnofacies.

20 This facies association is interpreted as having been deposited in a distal
21 burrowed lower shoreface to inner shelf setting based on its heterolithic
22 lithology, *Cruziana* ichnofacies (Figure 6-E) and the occurrence of combined
23 current and wave ripples. This suggests a low-energy, open-marine
24 environment in moderate water depths above storm wave base (SWB).

1

2 *HWFA7: Shelfal storm sheets*

3 Facies association HWFA7 is mostly composed of lithofacies HS and HM
4 (Figure 5). The thickness of these facies packages ranges from 0.3 to 18 m (1
5 and 59 ft). It is characterized by a continuously high GR response with values of
6 up to 150 API units or even higher . Where notably high GR peaks occur, these
7 may represent local flooding events interrupting a rather shallower depositional
8 sequence. This facies association has the lowest reservoir quality in the
9 formation with an average porosity of around 5% and an average horizontal
10 permeability of 0.2md.

11 It is interpreted to have been deposited in a distal shelf environment on the
12 basis of a high detrital clay content and the occurrence of combined wave and
13 current ripples (Figure 6-F). These suggest fluctuating energy levels in broadly
14 very low energy environment between the fair-weather wave base (FWWB) and
15 storm wave base (SWB). This is supported by the generally very low intensity of
16 bioturbation, the occasional occurrence of *Chondrites* burrows and shrinkage
17 cracks indicating deposition in a fairly distal, poorly oxygenated setting, perhaps
18 associated with distal waning storm events capable of transporting sand to the
19 open-marine shelf.

20 When core data was not available for several sections in the studied wells,
21 image log data was key to characterize the seven facies associations previously
22 mentioned (Figure 7).

23

24 **'NON-ACTUALISTIC' SEDIMENTARY MODEL**

25

1 Ever since James Hutton's key observations in the late eighteenth century,
2 modified by the work of John Playfair and, critically, Charles Lyell's
3 development of the concept of "uniformitarianism" in his Principles of Geology
4 (1832), geologists have sought to explain ancient processes by reference to
5 'actualistic' processes in order to better understand the sedimentary record.

6 However, the Earth has changed significantly through geological history.
7 Indeed, even from the early Paleozoic until present day, some processes and
8 depositional environments simply cannot be directly compared, since conditions
9 were significantly different. As Nichols (2017) certainly points out, if choosing a
10 'present' to be the 'key of the past' probably choosing the most recent 'present'
11 is not the best idea.

12 After careful study of the Hawaz Formation and the sedimentary processes
13 involved in its deposition, several significant concepts have been developed
14 which require further discussion in this respect (Table 2):

15 1) The lack of fauna and specifically flora in subaerial conditions during the
16 Middle Ordovician and more ancient times must have constituted a key
17 controlling factor on depositional processes operating in marginal marine
18 and coastal environments (Kenrick and Mitchell, 2015; Kenrick and Mitchell,
19 2016; Bradley et al., 2018). Firstly, vegetation constitutes a fixing element
20 within the substrate allowing the stabilization of floodplains and the control of
21 lateral river channel migration (Davies and Gibling, 2010; Davies et al.,
22 2011; Gibling and Davies, 2012), generally lowering the energy and net
23 sediment throughput of the environment. Whereas fluvial meandering
24 systems can be considered a general pattern in continental to marine
25 transitional zones for most present day cases (with the notable exception of

1 glacial-influenced settings or proximity to high relief source areas), the lack
2 of vegetation in the Middle Ordovician would have almost certainly
3 contributed to maintaining a high energy levels in the sedimentary system as
4 far as the coastal plain, characterized by laterally extensive braided
5 floodplains (Table 2).

6 The other remarkable aspect worthy of note is the effect of vegetation on the
7 generation of clay minerals (Table 2). Many Precambrian to Ordovician
8 clastic deposits are characterized by their low claystone or detrital clay
9 content. One of the reasons for this may be the absence of vegetation and
10 the resultant enhanced chemical weathering on land surfaces. The
11 generation of clays by weathering was significantly less than at the present
12 time, and therefore the availability of clays in the source areas, including
13 potentially erodible rocks, was also less for the same reason. Other
14 mechanisms for inputting a clay fraction into the depositional environment
15 may be associated with hydrothermal processes, diagenesis or volcanic ash
16 deposits; the latter has been identified by Marzo and Ramos (2003, personal
17 communication) and Ramos et al. (2006).

18 This is indeed what we see in the upper part of the Hawaz Formation;
19 typically comprising a package of sand prone tidal flat deposits with very few
20 clear claystone intervals, accumulating in a restricted low-energy
21 environment where, in a modern system, vegetation would fix finer
22 sediments at the very top of this kind of depositional succession.
23 Furthermore, the possibility of a clay input of volcanoclastic origin should not
24 be ruled out as Ramos et al., (2006) highlight the presence of K-bentonite
25 layers within the Hawaz Formation as observed in outcrops.

1 2) In line with Nichols (2017), the climate factor related to periods of
2 greenhouse and icehouse is also key in understanding how coastal
3 environments have evolved. Given that the last few million years of
4 geological history are considered as an icehouse period, some processes
5 related to the characteristic low relative sea levels are clearly not equivalent
6 to those produced during greenhouse periods, as much of the Cambrian-
7 Ordovician actually was. The relative sea level, during much of the
8 Ordovician (at least until the onset of the Hirnantian glaciation), was
9 probably tens of meters higher than at present time, which in the case study
10 would represent a very extensive area of land flooded, across a very low
11 relief cratonic margin (Table 2). Thus, confined estuary systems produced
12 by incised valleys during sea-level drop are not expected in this setting. This
13 discussion can be applied to the depositional model of the Hawaz
14 Formation. As such, classical estuarine environments are inherently unlikely.
15 Indeed, conventional lowstand systems tracts would be, in any case,
16 extremely difficult to identify, as major erosive features related to sea-level
17 drop would not be produced in this low gradient, cratonic transitional setting.

18 3) It is also relevant to our study that tidal range has not been constant through
19 the whole of Earth's history. Tides are largely controlled by differential
20 gravitational forces exerted between the Earth and the Moon, but the
21 distance between both bodies has changed through time at a currently
22 calculated rate of 3.8 cm/yr (1.5 in/yr) (Odenwald, 2018), entailing an
23 average Earth-Moon distance of 367,000 km (228,000 mi) as opposed to
24 384,000 km (238,000 mi) today. Tidal-energy dissipation over time is thus a
25 well-established process reflected in the increasing length of the day and

1 thus number of days per year. This appears to be a purely linear process
2 reflecting the progressive slowing of Earth's rotation and the associated
3 outward spiralling of the Moon. Thus, a day in the Ordovician is calculated to
4 have been 21 hours long and the year 414 days long. For our purposes it is
5 also true that the potential sediment load of nearshore tidal currents together
6 with their depositional effectiveness are related directly to the tidal range or
7 maximum tidal height (Williams, 2000); itself controlled by global tidal forces,
8 water depths and local topography. In general, therefore, we can assume
9 notably higher tidal ranges and more powerful tidal currents during the
10 deposition of the Hawaz Formation. Going further, we may also assume that
11 in the case of the upper Hawaz Formation, for example, even very small
12 variations in tidal range in such low gradient depositional environment would
13 result in a significant increase in the areal extension of marginal or paralic,
14 tidally influenced environments (Table 2).

15 4) Ichnofacies are usually related to sedimentary environments and,
16 particularly in tidal settings, there are specific parameters such as salinity,
17 depositional energy, sediment grain size and sedimentation rates that
18 control fauna colonization (Gingras, et al., 2012). However, there are some
19 ichnological assemblages, which may also have a chronostratigraphic value
20 when looked at on the basis of bioturbation intensity and lateral extent. A
21 very good example is the lower part of the Hawaz Formation and the
22 underlying Lower Ordovician Ash Shabiyat Formation, which are
23 characterized by their distinctive 'pipe rock' or high-density burrowed
24 *Skolithos* ichnofabric. Similarly, the association of this suspension-feeding
25 fabric, often overprinting a deposit feeding burrowing characterized by

1 common trilobite traces and thus a “true” *Cruziana* ichnofacies is distinctive.

2 Some if not many or even all of the organisms responsible for these

3 ichnofabrics are already extinct (Table 2). Thus, the occurrence of these

4 ichnofacies in such a very low gradient, cratonic platform is highly unlikely in

5 the present day.

6 After these comments, it is also worthwhile considering that the geomorphology

7 of clastic coastal depositional environments is closely linked to the relative

8 influence of waves and tides along the coastline (Harris and Heap, 2003), their

9 evolution controlled by three main factors: sediment supply, physical processes

10 (river currents, tidal currents and waves) and relative sea level variation

11 (Dalrymple, 1992, Boyd et al., 1992; Dalrymple et al., 1992; Harris et al., 2002).

12 Thus, taking all of this into account with and applying it to the study dataset in

13 the area, a ‘non-actualistic’ depositional model is proposed for the Hawaz

14 Formation based upon modern sedimentological criteria but constrained and

15 adapted to Middle Ordovician environmental conditions (Figure 8).

16 It was a constantly evolving tide-dominated environment, evolving from a

17 relatively open-marine setting characterized by mixed storm-tide-dominated

18 deposition towards a more protected subtidal to intertidal setting on an

19 embayed coastline. This promoted tides as the dominant controlling factor on

20 sedimentation process, supported by the vertical arrangement or stacking of

21 facies associations. It shows a lower shoreface to shelf environment with sandy

22 storm sheet deposits present across much of the basin. Above this lower

23 interval, a laterally extensive and fluvio-tidal to subtidal complex comprising of

24 tidal channels and bars developed across the study area (Figure 8-A). The

25 distal part of this subtidal complex eventually became abandoned as sea level

1 rose creating a system of lagoons and barrier islands (not clearly identified in
2 the subsurface) (Figure 8-B). Finally, prograding tidal flats developed during a
3 relative high sea level stage (Figure 8-C).

4 From subsurface paleocurrent data it is apparent that the depositional system
5 evolved from a coastal environment in the south-southeast to fully marine
6 environments towards the north-northwest. The data show only limited
7 dispersion defining a clear depositional trend from southeast to northwest with
8 strong ebb current indicators. These data are in accordance with those of
9 Ramos et al. (2006) from outcrops in the Gargaf high. Evidence of bidirectional
10 current indicators in primary sedimentary structures is, however, hard to
11 observe. Although the presence of this kind of feature would strongly support
12 an important tidal influence, it is not always present in many tidal deposits. On
13 the other hand, no evidence for a seasonally controlled river have so far been
14 found in the succession which would help to preserve this type of reverse flow
15 structure during periods of low fluvial regime (Dalrymple and Choi, 2007).
16 However, the presence of clay drapes in most of the lithofacies described does
17 strongly support an important tidal effect throughout the depositional system.

18

19 **SEQUENCE STRATIGRAPHY AND ZONATION OF THE HAWAZ** 20 **FORMATION**

21 The purpose of this section is to recognize and correlate stratigraphic surfaces
22 representing changes in depositional trends and to interpret the resulting
23 stratigraphic units bounded by these surfaces.

1 The key bounding surfaces splitting genetic sedimentary packages were
2 recognized using a material-based sequence stratigraphic approach (Embry,
3 2009). The defined surfaces are:

4 - **Maximum regressive surface**, where a conformable horizon marks a
5 change from coarsening and shallowing upwards to fining and deepening
6 upwards;

7 - **Maximum flooding surface**, where a conformable horizon marks a change
8 from fining and deepening upwards to coarsening and shallowing upwards
9 and is normally represented by the highest clay content in the succession;

10 - **Shoreline ravinement unconformity**, where a clear erosive surface is
11 overlain by brackish marine deposits and which represents erosion in the
12 stratigraphic unit produced by wave and tidal currents during an early
13 transgressive stage just after a base level fall;

14 - **Regressive surface of marine erosion**, where in an overall regressive
15 succession there is a clear change in depositional trend with shelfal deposits
16 abruptly overlain by prograding shoreface deposits. As suggested by Embry
17 (2009), this last surface, is not a suitable surface for correlation due to its
18 highly diachronous nature, so has not been used as a main bounding
19 surface for our sequence stratigraphic framework. However, locally it may be
20 of use in explaining trend changes in the facies succession observed in
21 some wells.

22 Several low-order and numerous high-order sequences can be recognized in
23 the stratigraphic record of the Hawaz Formation (Figure 9) but, after analyzing
24 the evolution or stacking of the facies associations in each well it is possible to
25 erect a simplified scheme with three major depositional sequences (DS1-3) and

1 5 Hawaz reservoir zones (HWZ1-5) each defined by key correlatable genetic,
2 material-based surfaces (Figure 9).

3 The top of the Ash Shabiyat Formation is marked by a sharp or slightly more
4 gradational shift from the blocky, low GR response, characteristic of this
5 formation, to a notably more spiky or serrate GR response typical of much of
6 the lower Hawaz. This shift is interpreted not only as a maximum regressive
7 surface but also as a sequence boundary. As such it is a compound surface
8 and might be considered in terms of marine erosion as a ravinement which
9 marks the base of the depositional sequence 1 (DS1) (Figure 9).

10 The overlying HWZ1 is broadly transgressive in character, comprising stacked
11 fining-upwards parasequences (including a regionally distinctive and extensive
12 abandoned subtidal complex) capped by a regional flooding surface (Figure 9),
13 and finally a cleaning-upwards, progradational parasequence or parasequence
14 set.

15 The boundary between HWZ1 and HWZ2 is marked in all the wells by an abrupt
16 change in lithology to more argillaceous facies recording a marked deepening in
17 the basin. This is an excellent and consistent correlatable surface but is not fully
18 genetic as the maximum flooding surface of the DS1, only rarely coincides with
19 the lithological change and is instead typically picked a short distance above the
20 shift at the highest GR peak in the well (Figure 9).

21 The maximum flooding surface defines the onset of the highstand systems tract
22 (HST) of DS1, which coincides completely with the zone HWZ2. This can often
23 be divided into two subzones (HWZ2a and HWZ2b) separated by a regressive
24 surface of marine erosion (Figure 9), created by the cut of waves and tides in
25 the lower shoreface during the regression of the shoreline. This surface

1 separates a dirty sandy package from a cleaner sandy package within a
2 coarsening-upwards parasequence or parasequence set as suggested by the
3 GR response and facies analysis. However, this surface is not easily
4 recognizable in all wells and has not been used as a regional correlative surface
5 due to its probable diachronous nature.

6 The HST of DS1 is truncated by an erosive surface interpreted as a shoreline
7 ravinement unconformity (Figure 9) generated by the action of wave and tidal
8 currents during an early transgressive stage just after a base level fall and
9 probably enhanced by an allocyclic trigger mechanism, perhaps tectonics
10 related. This surface would also be a sequence boundary and would
11 correspond with the onset of the depositional sequence 2 (DS2) and the base of
12 zone HWZ3, the main reservoir section of the Hawaz Formation. The facies
13 association immediately overlying this key boundary is usually HWFA2 (Subtidal
14 complex), considered to represent an early transgressive systems tract (TST)
15 equivalent to zone HWZ3. Locally, this zone shows minor higher frequency
16 flooding surfaces mostly composed of heterolithics (Figure 9). These flooding
17 surfaces could be interpreted as condensed lagoonal deposits, but the lack of
18 biostratigraphic data in this sand-prone package suggests we should treat this
19 hypothesis with caution, although the presence of these sub-environments
20 should not be rejected. Tidal inlet storm deposits or inclined heterolithic
21 stratification (IHS) could also be a plausible option, considering the broad
22 general subtidal setting of this zone.

23 The boundary between zones HWZ3 and HWZ4 is marked by a change in
24 depositional environment from a subtidal to intertidal setting. This boundary
25 would be close to the maximum flooding surface after which the tidal flat would

1 prograde infilling the available space (bay infilling) under a forced regression
2 pattern, whereas further to the north barrier island deposits (observed in Gargaf
3 outcrops by Ramos et al., 2006) would most likely have limited the connection
4 to the open sea.

5 Zone HWZ4 comprises stacked fining-upwards parasequences, mainly formed
6 by tidal sand to mixed flat deposits cut by tidal creeks (Figure 9). Similar
7 processes have been highlighted by Desjardins et al. (2012) in the lower
8 Cambrian Gog Group of the Canadian Rocky Mountains where tidal flats are
9 forced to regress in response to falling sea level in tide-dominated settings.

10 Above zone HWZ4, the depositional trend changes again and GR values begin
11 to decrease in response to increasingly abundant cleaner sand deposits. There
12 is no evidence of sharp changes either in lithology, or in conventional log
13 responses suggesting there is no major unconformity. However, some subtidal
14 packages are preserved sometimes at the very top of the Hawaz Formation
15 which would denote a new transgression. Thus, the boundary between HWZ4
16 and HWZ5 is considered to be a compound maximum regressive surface and
17 sequence boundary which would constitute the beginning of a rarely preserved
18 depositional sequence 3 (DS3) (Figure 9). Zone HWZ5 is often eroded and
19 overlain by the Upper Ordovician formations or the base of the Silurian.

20

21 **DISCUSSION**

22 Following Boyd et al. (1992) and Dalrymple et al. (1992), clastic coastal
23 depositional environments are classified on a ternary diagram summarizing the
24 main factors (rivers, waves and tides) controlling the geomorphology of linear
25 shorelines, deltas or estuaries. This is a very useful and powerful tool in

1 'actualistic' or 'near-actualistic' systems, but in many cases it might be hard to
2 apply to very ancient coastal to shallow marine depositional systems, notably
3 those of the Precambrian to lower Paleozoic due to major differences in Earth
4 surface dynamics. Nevertheless, while some of these ancient depositional
5 systems lack obvious modern analogues, some features remain comparable
6 with modern environments. A detailed interpretation from subsurface cores and
7 logs highlights the major depositional and paleogeographic factors responsible
8 for the Middle Ordovician Hawaz Formation of the northern Murzuq Basin. The
9 resultant seven correlatable facies associations (HWFA1 to HWFA7) and the
10 robust sequence stratigraphic framework suggest that the Hawaz Formation
11 was deposited in an intertidal to subtidal environment prograding from south to
12 north. The facies associations and their linked ichnogenera suggest that water
13 depths are unlikely to have exceeded several tens of meters (hundreds of feet),
14 with the sea floor above storm wave base at most locations.

15 Considering the significant areal extent, not only of the Hawaz Formation across
16 the Murzuq Basin but also its lateral equivalents, in both Kufra and Illizi Basins,
17 which lack the key unburrowed cross-bedded sandstones (McDougall et al.,
18 2008; McDougall et al., 2011) typical of the subtidal complex described in this
19 work, it is clear that deposition occurred in and on the margins of an epeiric sea
20 characterized by a very low bathymetric relief and very broad facies belts tracts.
21 Dalrymple and Choi (2007) suggest fluvio-tidal transition zones may range in-
22 width up to hundreds of kilometers (hundreds of miles) in low-gradient settings
23 as would indeed be the case for the northern margin of Gondwana during the
24 Middle Ordovician. In such environments small changes in relative sea level
25 would be sufficient to cause major lateral shifts in facies belts. These small

1 changes occurred during a greenhouse period with relatively high global sea
2 levels. There is no evidence of incised valley systems within the Hawaz
3 succession suggesting global sea level remained relatively high through its
4 deposition. As such, lowstand systems tract facies could not be observed either
5 in the Gargaf high outcrops (Anfray and Rubino, 2003), or in the subsurface of
6 the Murzuq Basin.

7 During the initial stages of sea-level rise (TST), coastal areas were slowly
8 flooded, producing subtidal sedimentation associated with fluvial discharge
9 along embayed coastlines, presumably due to flooding of braided fluvio-tidal
10 systems, whereas during stages of high sea levels (HST), the shoreline
11 migrated seaward, resulting in the progradation of tidal-wave influenced strand
12 plains, beaches, or deltas associated with gentle lobate to linear coasts. The
13 embayed morphology of coastal areas was probably enhanced by tectonism,
14 which controlled the size and subsidence of the basin, generating a large-scale
15 depressed area, elongated in an approximately north-south direction (Klitzsch,
16 2000). Such a large-scale embayment characterized by a very low gradient
17 probably increased tidal power (Ramos et al., 2006).

18 The vertical stacking of the facies association packages was principally
19 controlled by eustasy, as suggested by the presented zonation. However, there
20 are other secondary factors which almost certainly acted to control the evolution
21 of sedimentation in these coastal and shallow-marine environments, notably
22 subsidence and sediment supply (Dalrymple, 1992; Dalrymple et al., 1992;
23 Walker and Plint, 1992; Johnson and Baldwin, 1996).

24 Given that this environment was characterized by a very low gradient it is
25 possible that sedimentation was controlled by a pre-existing paleorelief

1 expressed as complex lobate to linear shoreline. The low gradient of this
2 depositional system impeded the development and identification of well-defined
3 clinoforms both in outcrops and in seismic images. What is evident is the
4 significant influence of tidal processes in these deposits with a preferential
5 paleocurrent direction towards the north-northwest according to both outcrop
6 (Ramos et al., 2006) and FMI data from wells showing some bi-directional
7 current indicators in some cases. In addition there is also strong evidence for a
8 secondary paleocurrent dispersal system flowing towards the northeast which
9 requires further study.

10 Several depositional models have been proposed for the Hawaz Formation. Vos
11 (1981) suggested a fan-delta complex as the more likely setting, whilst other
12 authors including Ramos et al. (2006) have argued for deposition within a
13 mega-estuary or tidal gulf setting. The current study strongly suggests that the
14 Hawaz Formation cannot be compared with any present day coastal
15 environment. The clear tidal influence observed in the system and the vertical
16 stacking of facies associations highlight the evolution of a shallow marine
17 environment from a subtidal to an intertidal setting accompanied by parallel
18 evolution of ichnofacies and fossil content (Figure 10).

19 The presence of some ichnogenera such as *Chondrites* in heterolithics from the
20 most distal facies associations HWFA6 and HWFA7, compared to those
21 deposited in the most proximal association HWFA1, suggests that a different
22 setting for the lower (DS1; HWZ1-2) and upper (DS2-3; HWZ3-5) parts of the
23 Hawaz Formation should be considered. Gibert et al. (2011) concluded that the
24 restricted and uncommon ichnofacies assemblage in the upper part of the
25 Hawaz was not clear. A mixed *Cruziana* and *Skolithos* ichnofacies has been

1 observed both in the subsurface and in outcrops, the latter showing many
2 excellent examples of trilobite traces (Ramos et al., 2006 and Gibert et al.,
3 2011). Some authors have realized that, although trilobite tracks typical of the
4 *Cruziana* ichnofacies are usually regarded as indicators of open-marine
5 offshore to nearshore settings, their presence in heterolithic facies can no
6 longer be taken as an absolute indicator of deposition in subtidal settings in the
7 early Paleozoic and indeed they may have been notably more common within
8 intertidal deposits than currently envisioned (Mángano et al., 2014). The 'non-
9 actualistic' sedimentary model presented in this study incorporates this
10 observation so that the *Cruziana* ichnofacies is also considered a common
11 characteristic element of shallow tidal flat settings (Figure 10).

13 CONCLUSIONS

14 Where encountered in the subsurface of the northern Murzuq, the Hawaz
15 Formation is represented by a clastic succession mainly comprising fine- to
16 locally medium-grained quartzarenites and subarkosic arenites, with
17 subordinate sublithic arenites, up to 210 m-thick (690 ft-thick). Fifteen major
18 lithofacies, comprising sandstones and heterolithics have been recognized and
19 grouped into seven correlatable facies associations. These include: (1) Tidal flat
20 (HWFA 1), (2) Subtidal complex (HWFA 2), (3) Abandoned subtidal complex
21 (HWFA 3), (4) Middle to lower shoreface (HWFA 4), (5) Burrowed shelfal and
22 lower shoreface (HWFA5), (6) Burrowed inner shelf (HWFA 6) and (7) Shelfal
23 storm sheets (HWFA7), all deposited within the framework of an intertidal to
24 subtidal setting.

1 There is a clear relationship between facies and reservoir quality for the Hawaz
2 Formation. The best reservoir quality sandstones are those comprising facies
3 association HWFA2 (subtidal complex) with an average porosity of 11% and
4 horizontal permeability of 125md and general absence of thick mud drapes and
5 interlayered claystones.

6 The depositional model for the Hawaz Formation cannot be compared with an
7 'actualistic' sedimentary analogue due to the major differences stemming from:
8 a) the absence of fauna and especially flora in subaerial environments which
9 directly determines coastal dynamics; b) the difference in relative sea level and
10 its control on erosion in shallow marine settings together with the low gradient
11 depositional setting which promoted very wide facies belts compared to most
12 present day moderate to high gradient depositional systems; c) the difference in
13 tidal ranges reflecting the progressive change in the distance between the Earth
14 and the Moon, and finally; d) the characteristic ichnofacies observed in the
15 Hawaz are not present in modern environments.

16 The Hawaz Formation can be divided into three main depositional sequences
17 (DS1-3), each with characteristic systems tracts bounded by key surfaces:
18 maximum regressive surface, maximum flooding surface and unconformable
19 shoreline ravinement surface.

20 Based upon this systems tracts architecture, a genetic zonation composed of 5
21 zones has been proposed (HWZ1 to HWZ5). This new stratigraphic zonation
22 should serve as a useful tool to improve the management in oil production from
23 the Hawaz Formation. The Hawaz Formation extends laterally hundreds of
24 kilometers (hundreds of miles) away from the study area forming an excellent
25 regional reservoir across the Murzuq and southern Ghadames (Berkine) Basins

1 and, to a lesser extent, as the laterally equivalent unit III in the Illizi Basin. The
2 facies schemes, depositional model and zonation framework proposed here
3 should also be applicable to existing or potential Hawaz reservoirs elsewhere
4 within this larger region.

5

6

7 REFERENCES

8

9 Abouessa, A., 2012, Diagenetic properties of Hawaz Formation, Murzuq Basin,
10 Libya. In: M.J. Salem, M.T. Elbakai & Y. Abutarruma (eds), *The Geology of*
11 *Southern Libya*. Earth Sc. Soc. of Libya, Tripoli, v. 1, p. 47-82.

12 Abouessa, A. and Morad, S., 2009, An integrated study of diagenesis and
13 depositional facies in tidal sandstones: Hawaz Formation (Middle
14 Ordovician), Murzuq Basin, Libya. *J. Petrol. Geology*, v. 32, pp. 39-66.

15 Anfray, R. and Rubino, J-L., 2003, Shelf Depositional Systems of the Ordovician
16 Hawaz Formation in the Central Al Qarqaf High. In: Salem, M.J. & Oun, K.M
17 (Eds) *The Geology of Northwest Libya II*. Gutenberg Press, Malta, p. 123-
18 134.

19 Aziz, A., 2000, Stratigraphy and hydrocarbon potential of the Lower Paleozoic
20 succession of License NC-115, Murzuq Basin, SW Libya, in M. A. Sola and
21 D. Worsley, eds., *Geological exploration in Murzuq Basin*: Amsterdam,
22 Elsevier Science, p. 349–368.

23 Boote, D.R.D, Dardour, A., Green, P. F., Smewing, J. D., Van Hoeflaken, F.,
24 2008, Burial and Unroofing History of the Base Tanezzuft 'Hot' Shale Source
25 Rock, Murzuq Basin, SW Libya: New AFTA Constraints from Basin Margin
26 Outcrops (abs.). Paper presented at the 4th Sedimentary Basins of Libya
27 Symposium: the Geology of Southern Libya, 17-20 November, Tripoli, Libya.

28 Boyd, R., Dalrymple, R., Zaitlin, B. A., 1992, Classification of clastic coastal
29 depositional environments: *Sedimentary Geology*, v. 80, p. 139–150.

- 1 Bradley, G., Redfern, J., Hodgetts, D., George, A. D., Wach, G. D., 2018, The
2 applicability of modern tidal analogues to pre-vegetation paralic depositional
3 environments. *Sedimentology*, v. 65, p. 2171-2201.
- 4 Dalrymple, R. W., 1992, Tidal depositional systems, in R. G. Walker and N. P.
5 James, eds., *Facies models. Response to sea level change*:
6 Waterloo, Geological Association of Canada, p. 195–218.
- 7 Dalrymple, R. W., Zaitlin, B. A., Boyd, R., 1992, Estuarine facies models:
8 Conceptual basis and stratigraphic implications: *Journal of Sedimentary*
9 *Petrology*, v. 62, p. 1130–1146.
- 10 Dalrymple, R. W. and Choi, K., 2007, Morphologic and facies trends through
11 the fluvial-marine transition in tide-dominated depositional systems: A
12 schematic framework for environmental and sequence-stratigraphic
13 interpretation. *Earth –Science Reviews*, v.81, p.135-174.
- 14 Davidson, L., Beswetherick, S., Craig, J., Eales, M., Fisher, A., Himmali, A.,
15 Jho, J., Mejrab, B., Smart, J., 2000, The structure, stratigraphy and
16 petroleum geology of the Murzuq Basin, southwest Libya, in M. A. Sola and
17 D. Worsley, eds., *Geological exploration in Murzuq Basin*: Amsterdam,
18 Elsevier Science, p. 295–320.
- 19 Davies, N. S. and Gibling, M. R., 2010, Cambrian to Devonian evolution of
20 alluvial systems: The sedimentological impact of the earliest land plants.
21 *Earth Science Reviews*, v. 98, p. 171-200.
- 22 Davies, N. S., Gibling, M. R., Rygel, M. C., 2011, Alluvial facies evolution during
23 the Palaeozoic greening of the continents: case studies, conceptual models
24 and modern analogues. *Sedimentology*, v. 58, p. 220-258.
- 25 Desjardins, P.R., Buatois, L. A., Pratt, B. R., Mángano, M. G., 2012, Forced
26 Regressive Tidal Flats : Response to Falling Sea Level in Tide-dominated
27 Settings. *Journal of Sedimentary Research*, v. 82, p. 149-162.
- 28 Embry, A., 2009, *Practical Sequence Stratigraphy*. Canadian Society of
29 Petroleum Geologists, 79 p.

- 1 Fello, N.; Lüning, S.; Storch, P.; Redfern, J., 2006, Identification of early
2 Llandovery (Silurian) anoxic palaeo-depressions at the western margin of
3 the Murzuq Basin (southwest Libya), based on gamma-ray spectrometry in
4 surface exposures. *GeoArabia*, v. 11, p. 101-118.
- 5 Franco, A., Perona, R., Dwyianti, R., Yu, F., Helal, S., Suarez, J., Ali, A., 2012,
6 NC186 Block, Murzuq Basin: Lessons Learned from Exploration. In: M.J.
7 Salem, I.Y. Mriheel & A.S. Essed (eds.), *The Geology of Southern Libya*.
8 Earth Sc. Soc. of Libya, Tripoli, v. 2, p. 37-50.
- 9 Ghienne, J.-F., Deynoux, M., Manatschal, G., Rubino, J.-L., 2003,
10 Palaeovalleys and fault-controlled depocentres in the Late-Ordovician glacial
11 record of the Murzuq Basin (central Libya). *Comptes Rendus Geoscience*, v.
12 335, p. 1091–1100.
- 13 Gibert, J.M., Ramos, E., Marzo, M., 2011, Trace fossils and depositional
14 environments in the Hawaz Formation, Middle Ordovician, western Libya.
15 *Journal of African Earth Sciences*, v. 60, p. 28–37.
- 16 Gibling, M. R. and Davies, N. S., 2012, Palaeozoic landscapes shaped by plant
17 evolution. *Nature Geoscience*, v. 5, p. 99-105.
- 18 Gingras, M. K., MacEachern, J. A., Dashtgard, S. E., 2012, The potential of
19 trace fossils as tidal indicators in bays and estuaries. *Sedimentary Geology*,
20 v. 279, p. 97-106.
- 21 Hall, P.B., Bjorøy, M., Ferriday, I.L., Ismail, Y., 2012, Murzuq Basin Source
22 Rocks. In: M.J. Salem, I.Y. Mriheel & A.S. Essed (eds) *The Geology of*
23 *Southern Libya*. Earth Sc. Soc. of Libya, Tripoli, v. 2, p. 63-84.
- 24 Hallet, D., 2002, *Petroleum geology of Libya*: Amsterdam, Elsevier, 503 p.
- 25 Harris, P. T., Heap, A. D., Bryce, S. M., Porter-Smith, R., Ryan, D. A., Heggie,
26 D. T., 2002, Classification of Australian clastic coastal depositional
27 environments based upon a quantitative analysis of wave, tidal, and river
28 power: *Journal of Sedimentary Research*, v. 72, p. 858–870.

- 1 Harris, P. T. and Heap, A. D., 2003, Environmental management of clastic
2 coastal depositional environments: inferences from an Australian
3 geomorphic database. *Ocean & Coastal Management*, v.46, p. 457-478.
- 4 Johnson, H. D. and C. T. Baldwin, 1996, Shallow clastic seas, in H. G. Reading,
5 ed., *Sedimentary environments: Processes, facies and stratigraphy*: Oxford,
6 Blackwell Science, p. 232–280.
- 7 Kenrick, P. and Mitchell, R. L., 2015, The origins of land plants communities.
8 The rise and fall of photosynthate: Evolution of plant/fungus interactions from
9 paleobotanical and phylogenomic perspectives Symposium.
- 10 Kenrick, P. and Mitchell, R. L., 2016, The early fossil record of land plants and
11 their environment. 38th New Phytologist Symposium – Colonization of the
12 terrestrial environment 2016, Bristol.
- 13 Klitzsch, E. H., 2000, The structural development of the Murzuq and Kufra
14 basins- Significance for oil and mineral exploration, in M. A. Sola and D.
15 Worsley, eds., *Geological exploration in Murzuq Basin*: Amsterdam, Elsevier
16 Science, p. 143–150.
- 17 D. P. Le Heron, O. Sutcliffe, K. Bourgig, J. Craig, C. Visentin, R. Whittington,
18 2004, Sedimentary architecture of Upper Ordovician tunnel valleys, Gargaf
19 Arch, Libya: implications for the genesis of a hydrocarbon reservoir
20 *GeoArabia*, v. 9, p. 137-160.
- 21 Lyell, C., 1832. *Principles of Geology* vol.II, John Murray, London.
- 22 Mángano, M. G., Buatois, L. A., Astini, R., Rindsberg, A. K., 2014, Trilobites in
23 early Cambrian tidal flats and landward expansion of the Cambrian
24 explosion. *Geology*, v.42, p. 143-146.
- 25 McDougall, N. and Martin, M., 2000, Facies models and sequence stratigraphy
26 of Upper Ordovician outcrops in the Murzuq Basin, SW Libya. *In*: M.A. Sola
27 & D. Worsley (eds). *Geological Exploration in Murzuq Basin*. Elsevier,
28 Amsterdam, p. 223-236.
- 29

- 1 McDougall, N. D., Gerard, J., Wloszczowski. D., and Sharky, K., 2008,
2 Ordovician Plays on the Arabian and Saharan Platforms: A Comparison;
3 Poster & Abstract; for AAPG International Conference & Exhibition; Cape
4 Town, South Africa.
- 5 McDougall, N.D., Bellik, M and Jauregui, J. M..2011, Sedimentology and
6 sequence stratigraphy of the Ordovician section in the Gassi-Touil-Gassi
7 Chergui-In Amedjane area. Poster & Abstract; 5th Algerian Oil & Gas Energy
8 Week, Oran, Algeria.
- 9 Nichols, G., 2017, Challenging orthodoxy: is the Present the Key to the Past?
10 The Sedimentary Record, v. 15, no. 3, p 4-9.
- 11 Odenwald, S., 2018, Spacemath@NASA, <https://spacemath.gsfc.nasa.gov/>
12 (accessed Fefbruary 2, 2018).
- 13 Ramos, E., Marzo, M., Gibert, J.M.de, Tawengi, K.S., Khoja, A.A., Bolatti, N.D.,
14 2006, Stratigraphy and sedimentology of the Middle Ordovician Hawaz
15 Formation (Murzuq Basin, Libya). AAPG Bulletin, v. 90, p. 1309–1336.
- 16 Rider, M., 2004, *The Geological Interpretation of Well Logs*. Rider – French
17 Consulting Ltd.
- 18 Shalbak, F., 2015, *Paleozoic petroleum systems of the Murzuq Basin, Libya*.
19 Universitat de Barcelona, 203p.
- 20 Vos, R. G., 1981, Sedimentology of an Ordovician fan delta complex, western
21 Libya: Sedimentary Geology, v. 29, p. 153–170.
- 22 Walker, R. G. and A. G. Plint, 1992, Wave- and storm-dominated shallow
23 marine systems, in R. G. Walker and N. P. James, eds., Facies models.
24 Response to sea level change: Waterloo, Geological Association of Canada,
25 p. 219–238.
- 26 Williams, G. E., 2000, Geological constraints on the Precambrian history of
27 Earth's rotation. Reviews of Geophysics, v. 38, no. 1, p. 37–59.

1 **AUTHORS VITAE**

2 **Marc Gil Ortiz** ~ Marc Gil Ortiz is currently working as a Clastic Sedimentologist
3 in the Stratigraphy and Sedimentology Team of Repsol Exploración. He is a
4 member of the Geomodels Research Institute and researcher of the University
5 of Barcelona where currently he is also doing his PhD. His research is mainly
6 focused on clastic sedimentology, sequence stratigraphy and the relationships
7 between tectonics and sedimentation.

8 **Neil David McDougall** ~ Neil McDougall was awarded his Ph.D in geology at
9 the University of Liverpool in 1988. Since then he has worked as a Senior
10 Sedimentologist for Robertson Research and as a Clastic Sedimentologist
11 Advisor for Repsol Exploración. He has studied clastic reservoirs in various
12 basins worldwide with a special focus on the Lower Paleozoic of Libya and
13 Algeria.

14 **Patricia Cabello** ~ Patricia Cabello is a lecturer at the University of Barcelona
15 and is a member of the Geomodels Research Institute and the Research Group
16 of Geodynamics and Basin Analysis. She received her Ph.D. from the
17 University of Barcelona in 2010. Her research is mainly focused on the
18 characterization of reservoirs and outcrop analogues.

19 **Mariano Marzo** ~ Mariano Marzo is a professor of stratigraphy at the University
20 of Barcelona. His research interest focuses on the application of clastic
21 sedimentology, sequence stratigraphy, reservoir modelling, and basin analysis
22 to the exploration and production of hydrocarbons. He has been involved in
23 several research projects funded by oil companies in southern Europe, the
24 North Sea, South America, and northern Africa.

25 **Emilio Ramos** ~ Emilio Ramos was awarded his Ph.D. in geology at the
26 University of Barcelona in 1988. Since then, he has held a post as a lecturer in
27 basin analysis and petroleum geology at the same university. He has worked on
28 several research projects on sedimentology and basin analysis in Spain, North
29 Africa, Antarctica, and South America.

30

1 FIGURES AND TABLE CAPTIONS

2 **Figure 1.** – Geological map of Libya showing the main sedimentary basins. The
3 Murzuq Basin is bounded by the Atshan arch to the northwest, the Gargaf high
4 to the north, the Tihemboka high to the southwest and the Tibesti high to the
5 southeast. The area of interest represented in Figure 3-A is highlighted in the
6 red box. Modified from Marzo and Ramos (2003, personal communication).

7 **Figure 2.** – A) Stratigraphic chart summarizing the stratigraphic column for the
8 Murzuq Basin highlighting the main stratigraphic units (1= Cambro-Ordovician;
9 2= Silurian; 3= Devonian-Carboniferous; 4= Mesozoic) and major basin-scale
10 unconformities. B) Wheeler diagram showing lithostratigraphic to
11 chronostratigraphic relationships of the Ordovician and Lower Silurian
12 succession in the area of study. C) Seismic line showing the typical
13 geomorphological signature of the Ordovician succession in form of paleohighs
14 ('buried hills') and paleovalleys. Silur. = Silurian; Dev. = Devonian; Carbonif. =
15 Carboniferous; Perm. = Permian; Q = Quaternary. The main petroleum systems
16 elements are also represented in Figure 2-A and B.

17 **Figure 3.** – (A) Satellite image of the northern Murzuq Basin highlighting the
18 study area (red box). (B) Study area showing the position of the wells. Find
19 highlighted the wells with core data available and, in white, the wells from
20 figures 4, 6, 7, 9 and 10. Note the distance between the studied area in the
21 subsurface and the western Gargaf high where the outcrops studied by Ramos
22 et al. (2006), referred to in this paper, are located.

23 **Figure 4.** – Core sections (90cm [35 in] length approx.) of the main lithofacies
24 identified in this study. Sx1= Large scale cross-bedded sandstones; Sx2 =
25 Small to medium scale cross-bedded sandstones; SI = Parallel-laminated
26 sandstones; Sxl = Cross-laminated sandstones; Sr = Ripple cross-laminated
27 sandstones; Sv = Massive sandstones; Sxb = Burrowed cross-bedded
28 sandstones; Sxlb = Burrowed cross-laminated sandstones; Srb = Burrowed
29 ripple cross-laminated sandstones; Sb = Burrowed sandstones with
30 Siphonichnus; MSb = Burrowed sandstones with feeding ichnofauna; HS =
31 Sandy heterolithics; HSb = Burrowed sandy heterolithics; HM = Muddy
32 heterolithics; HMb = Burrowed muddy heterolithics. See the location of the
33 corresponding wells (B, C, D, E, F and G) in Figure 3-B.

34 **Figure 5.** – Summary of facies associations and interpreted depositional
35 settings. Description includes typical core sections and thickness ranges. See
36 also the main lithofacies composing each facies association and the location of
37 detailed features shown in Figure 6. Interpretation in terms of depositional
38 environment is also included. In addition, summary conventional core analysis
39 (CCA) porosity (\emptyset) and permeability (K), data for every facies association and
40 average gamma-ray values are also shown. The last column shows the

1 sequence stratigraphic interpretation plus the location of each association within
 2 the depositional model of the Figure 8. Sx1= Large-scale cross-bedded
 3 sandstones; Sx2 = Small- to medium-scale cross-bedded sandstones; SI =
 4 Parallel-laminated sandstones; Sxl = Cross-laminated sandstones; Sr = Ripple
 5 cross-laminated sandstones; Sv = Massive sandstones; Sxb = Burrowed cross-
 6 bedded sandstones; Sxlb = Burrowed cross-laminated sandstones; Srb =
 7 Burrowed ripple cross-laminated sandstones; Sb = Burrowed sandstones with
 8 Siphonichnus; MSb = Burrowed sandstones with feeding ichnofauna; HS =
 9 Sandy heterolithics; HSb = Burrowed sandy heterolithics; HM = Muddy
 10 heterolithics; HMb = Burrowed muddy heterolithics. TST = transgressive
 11 systems tract; HST = highstand systems tract;

12 **Figure 6.** – Detailed close-up views of some characteristic sedimentary
 13 structures and fabrics of the Hawaz Formation in core. A) Mud-draped (flaser)
 14 lamination (arrows) in HWFA1 tidal flat facies association from well E. B)
 15 Mudstone rip-up clasts (arrows) from fluvio-tidal to subtidal channels of HWFA2
 16 subtidal complex in well F. C) Clay-draped current ripples (small arrows) from
 17 HWFA2 subtidal complex from well C. Notice the direction of the paleocurrent
 18 flow leftwards (horizontal arrow). D) Burrowed sandstones with characteristic
 19 *Skolithos* ichnofacies of the HWFA5 burrowed shelfal and lower shoreface
 20 facies association in well E. E) Characteristic view of the HWFA6 burrowed
 21 inner shelf deposits from well D. F) Clay-draped combined flow ripples (small
 22 arrows) from HWFA7 shelfal storm sheets in well D. Notice the direction of the
 23 paleocurrent flow rightwards in the upper part and bidirectional in the lower part
 24 of the image (horizontal arrows). See the location of the corresponding wells (C,
 25 D, E and F) in Figure 3-B.

26 **Figure 7.** – Representative sections of slabbed cores (40cm [~16 in]) for each
 27 facies association and a typical high-resolution formation microimager (FMI)
 28 image (3m [~10 ft] long) showing their main characteristics. From top left to
 29 bottom right: HWFA1 tidal flat, HWFA2 Subtidal complex, HWFA3 abandoned
 30 subtidal complex, HWFA4 middle to lower shoreface, HWFA5 burrowed shelfal
 31 to lower shoreface, HWFA6 bsponding wells (A, C, D and E) in Figure 3-B.

32 **Figure 8.** – Evolutionary sedimentological model for the deposition of the
 33 Hawaz Formation. A) Early transgressive systems tract highlighting
 34 embayments; B) Late transgressive systems tract; C) Highstand systems tract.
 35 The main facies associations are represented in the sketches. The sketches are
 36 purely conceptual but consistent with observed trends in the study area but not
 37 geographically tied to well data. Mean sea level = msl.

38 **Figure 9.** – Composite section of a well showing a synthetic stratigraphic
 39 column of the Hawaz Formation, the wireline log responses, the suggested
 40 zonation for the reservoir based on the facies associations and sequence
 41 stratigraphic framework. The Transgressive and Regressive stacking patterns

1 are represented on the figure together with the 3 main depositional sequences.
2 See the location of the corresponding well (B) in Figure 3-B.

3 **Figure 10.** – Three-dimensional conceptual sketch of a coastal tidal-influenced
4 environment analogue to the Hawaz Formation deposition during a highstand
5 systems tract stage, grading from a braided coastal plain environment in the
6 most proximal part of the sedimentary system to intertidal and subtidal
7 environments and lower shoreface to inner shelf settings. Note the clear
8 relationship between the ichnofacies assemblage and the energy of the
9 depositional environment. From left to right: (A) mixed *Cruziana* and *Skolithos*
10 ichnofacies assemblage with characteristic vertical suspension feeder burrows
11 of *Skolithos* (Sk) overprinting an ichnofabric comprising horizontal deposit
12 feeders and miners such as *Thalassionides* (Th) and *Planolites* (Pl) associated
13 with tidal flat deposits; (B) characteristic *Skolithos* ‘Pipe Rock’ ichnofacies with
14 typical *Siphonichnus* (Si) burrows from lower shoreface to burrowed shelfal
15 deposits; (C) Mixed *Cruziana* and *Skolithos* ichnofacies assemblage, from
16 burrowed inner shelf sediments with characteristic *Teichichnus* (Te),
17 *Thalassinoides* (Th) and *Skolithos* (Sk) burrows; (D) heterolithic mudstones
18 belonging to the most distal storm deposits with *Chondrites* (Ch) burrows
19 characteristic of the distal *Cruziana* ichnofacies. See the location of the
20 corresponding well (E and D) in Figure 3-B.

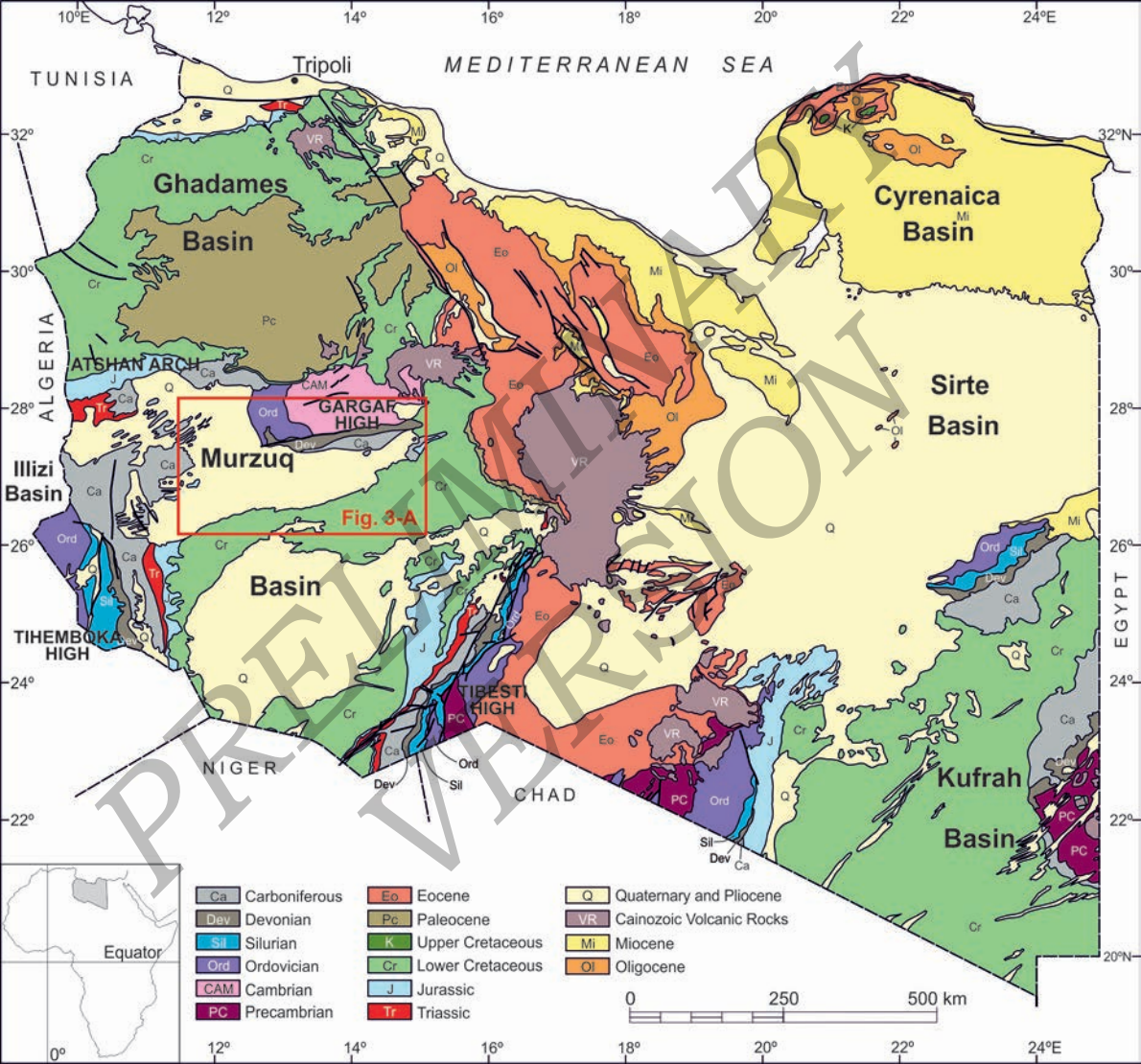
21

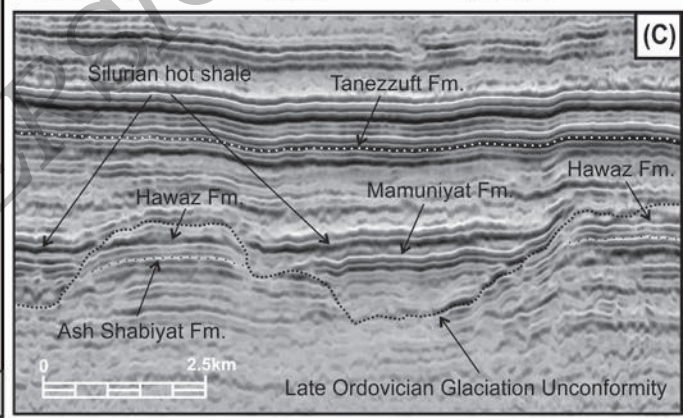
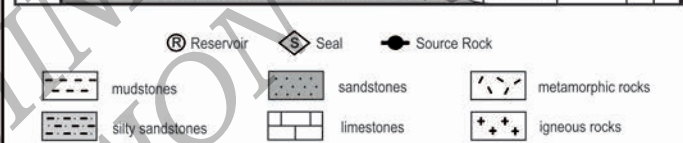
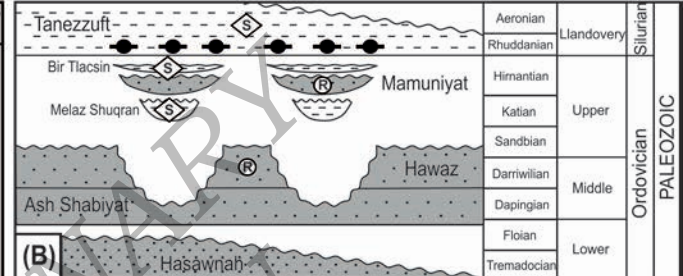
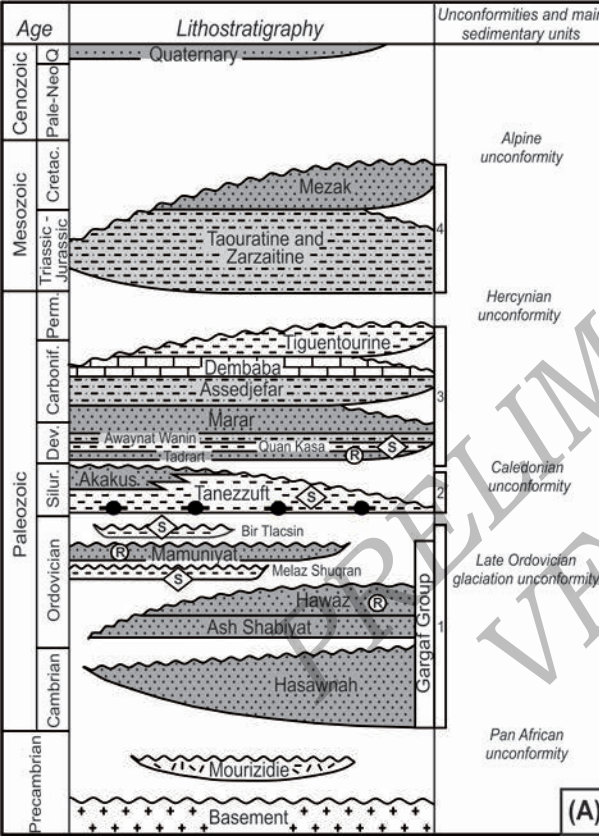
22 **Table 1.** – Lithofacies scheme for the Hawaz Formation.

23 **Table 2.** – Comparative table between key ‘actualistic’ (Present) and ‘non-
24 actualistic’ (early Paleozoic and older) main processes or controlling factors
25 affecting the geological signature of tidal-influenced successions in the
26 geological record.

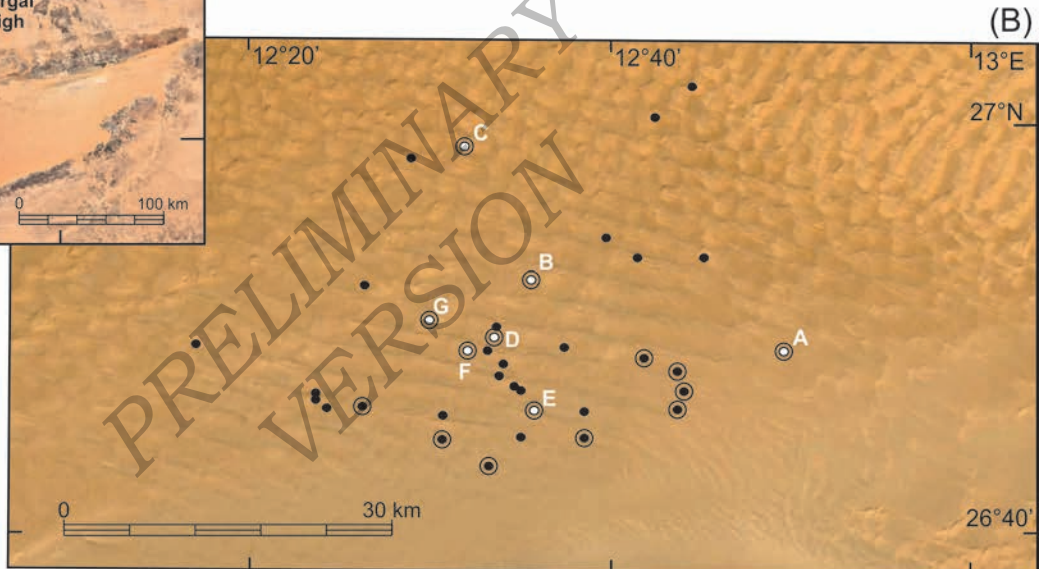
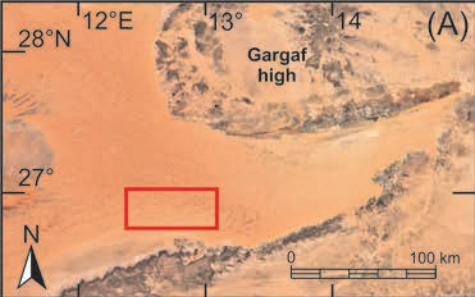
27

28

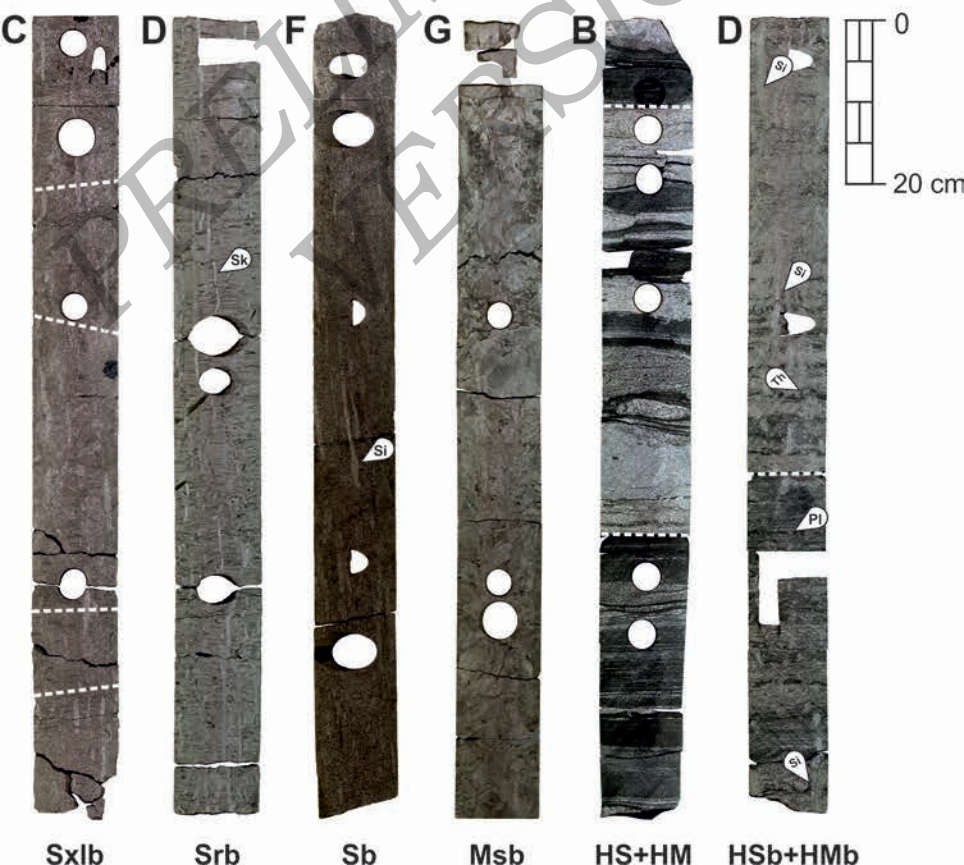
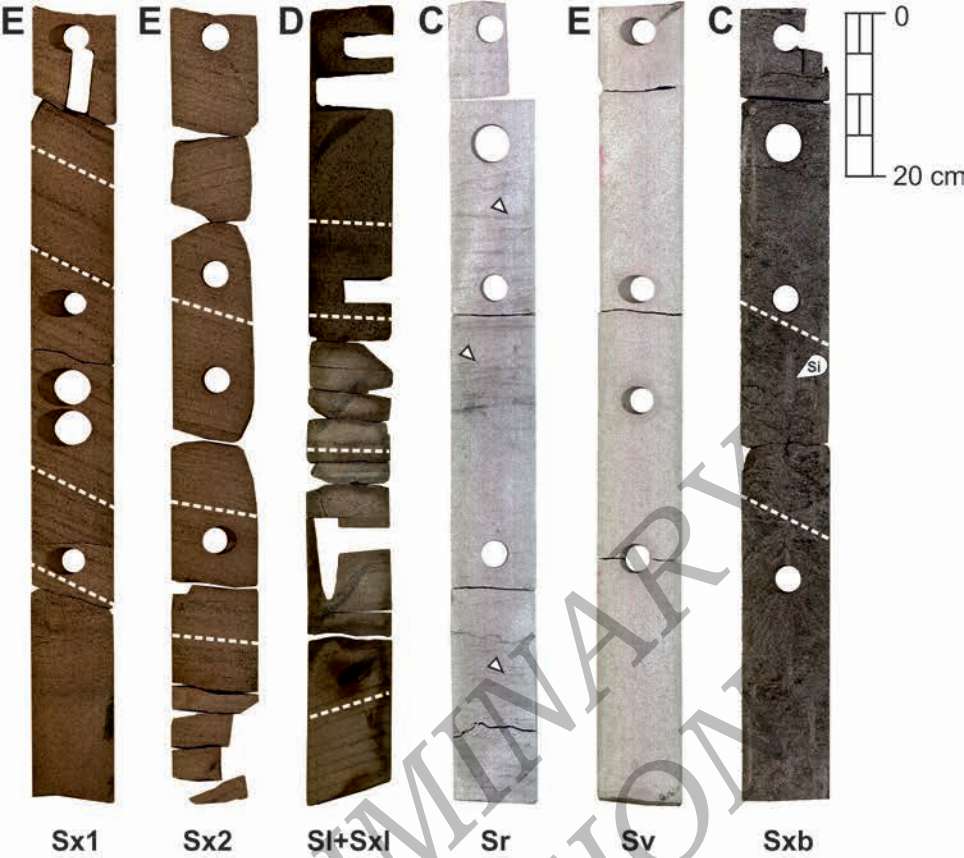


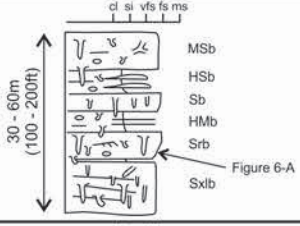
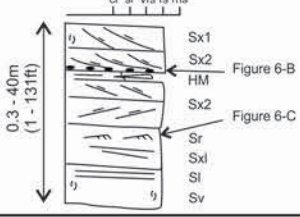
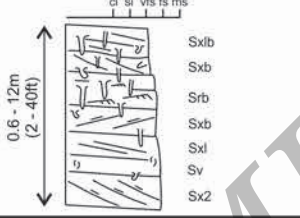
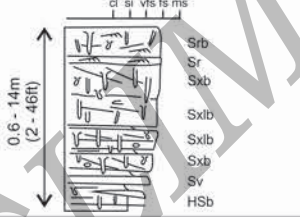
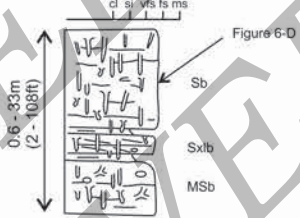
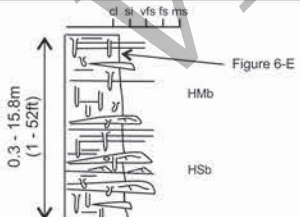
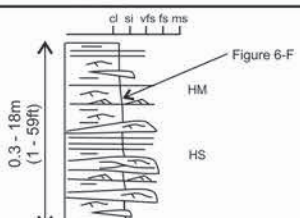


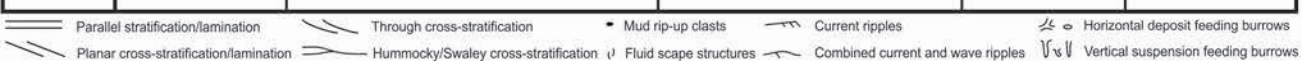
| Period | Stage | Sub-period | Period |
|------------|-------------|------------|-----------|
| Silurian | Llandovery | Upper | PALEOZOIC |
| | Rhuddanian | | |
| Ordovician | Katian | Middle | |
| | Darriwilian | | |
| Ordovician | Dapingian | Lower | |
| | Floian | | |
| Ordovician | Tremadocian | | |

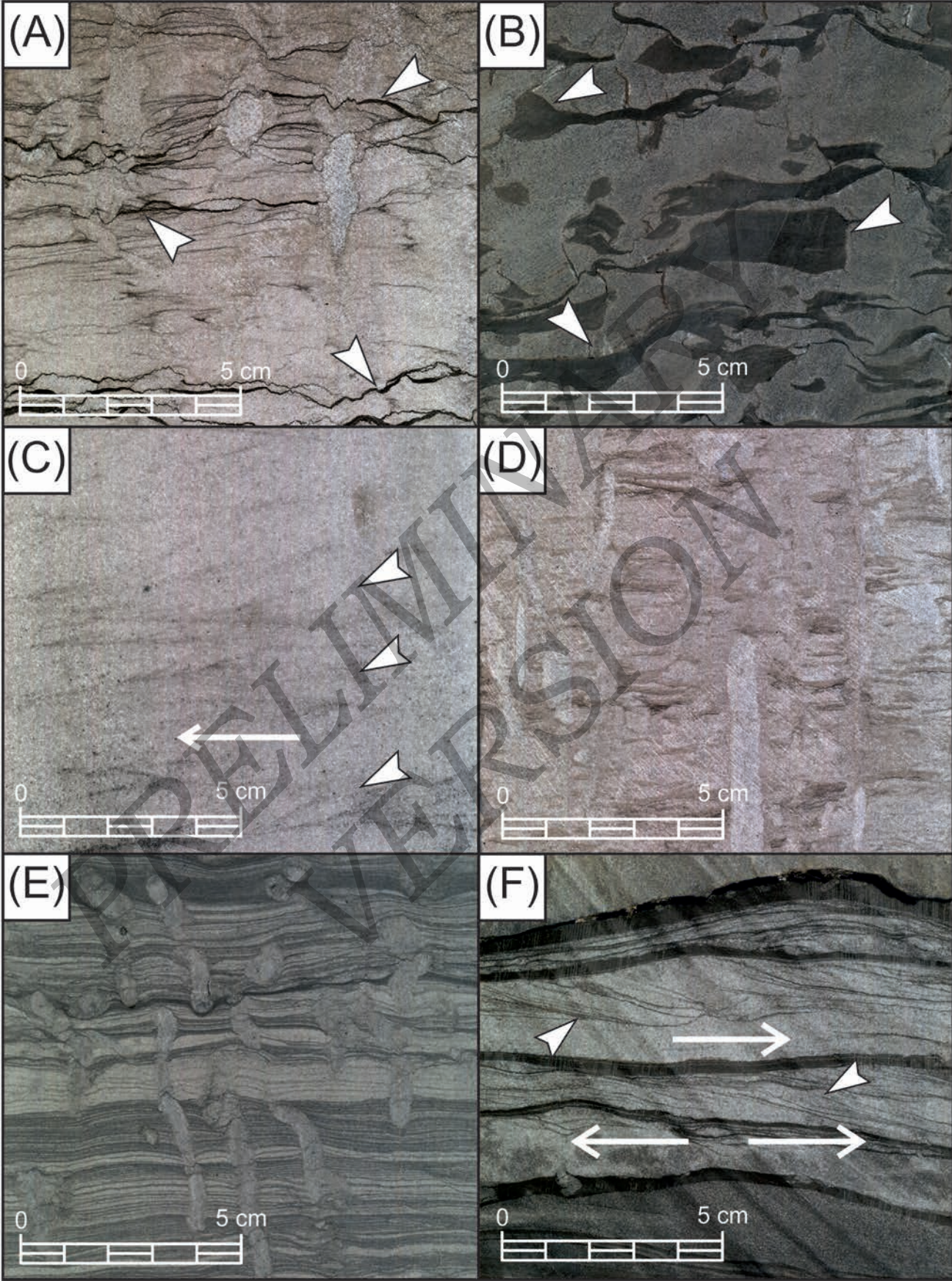


- Hawaz wells
- Hawaz wells (core data)
- Hawaz wells (Fig 4,6,7, 9 and 10)



| Depositional setting | Facies association | Description (Typical section with lithofacies & thickness ranges) | Interpretation | CCA average Ø / K Gamma Ray | Systems Tracts in Figure 8 |
|--|--|---|--|--------------------------------|--|
| FORESHORE Intertidal zone | HWFA1 Tidal flat |  | Tidal sand to mixed flat deposited during high relative sea levels in an embayed tidal-influenced setting | 13% / 30.4md 30 - 140 API | HST (Figure 8-C) |
| | HWFA2 Subtidal complex |  | Amalgamated complex of sand bars, dunes and channel deposits deposited in a fluvio-tidal to subtidal setting | 11% / 125md 25 - 65 API | Early and late TST (Figure 8-A & B) |
| MIDDLE SHOREFACE Subtidal zone | HWFA3 Abandoned subtidal complex |  | Distal equivalent of the subtidal complex product of the abandonment of previously active subtidal channels | 14% / 152md 25 - 70 API | Early and late TST (Figure 8-A & B) |
| | HWFA4 Middle to lower shoreface |  | Prograding middle to lower shoreface related to regressive sand belts during highstand sea level conditions | 14% / 56md 30 - 80 API | HST (Figure 8-C) |
| LOWER SHOREFACE below MFWB | HWFA5 Burrowed shelfal and lower shoreface |  | Deposition in a relatively protected to more open lower shoreface to inner shelf setting | 14% / 3.5md 30 - 80 API | Early TST, late TST and HST (Figure 8-A, B & C) |
| | HWFA6 Burrowed inner shelf |  | Deposition in an open-marine inner shelf setting | 9% / 0.2md 60 - 120 API | Late TST and HST (Figure 8-B & C) |
| | HWFA7 Shelfal storm sheets |  | Distal mixed sand to mud rich deposits product of waning storm events in an open-marine shelf setting | 5% / 0.2md 80 - 160 API | Early TST, late TST and HST (Figure 8-A, B & C) |

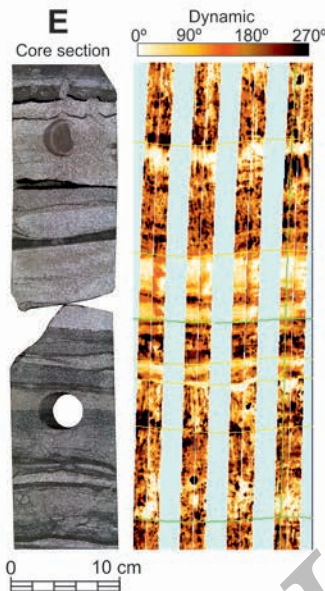




HWFA1
Tidal flat

HWFA2
Subtidal complex

HWFA3
Abandoned subtidal complex



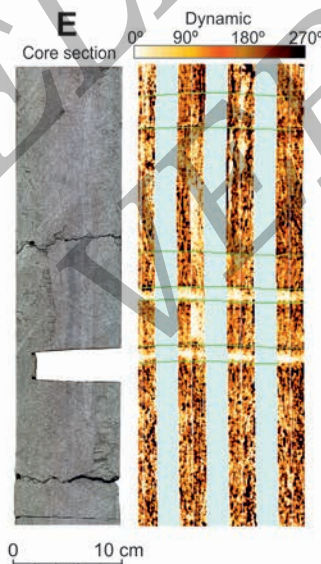
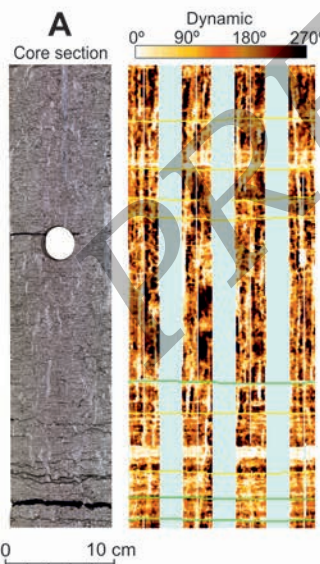
Core to FMI
not to same scale

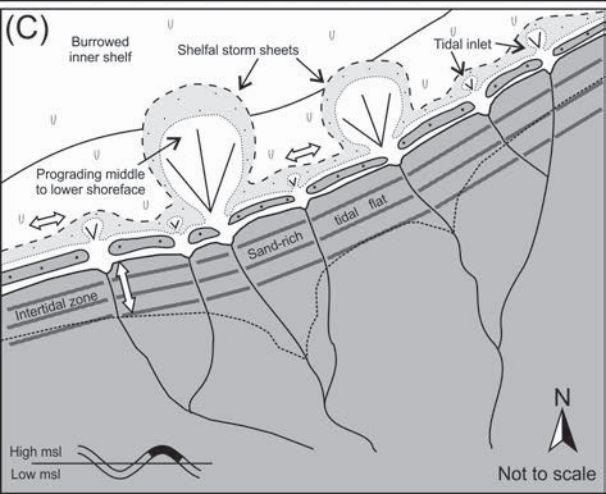
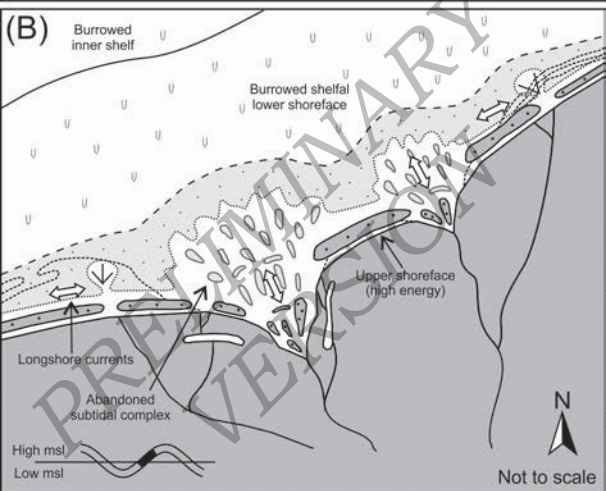
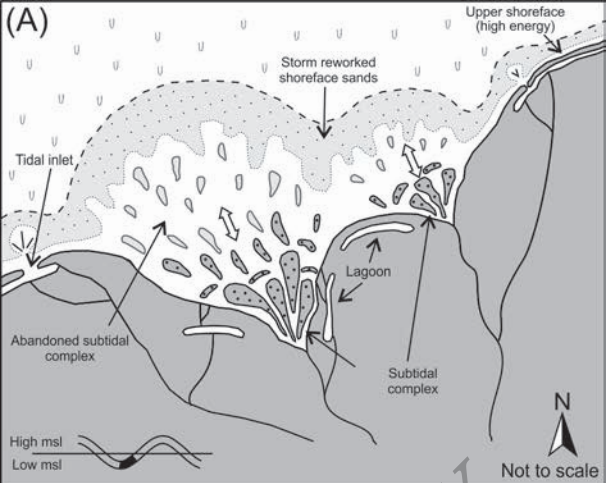
HWFA4
Middle to lower shoreface

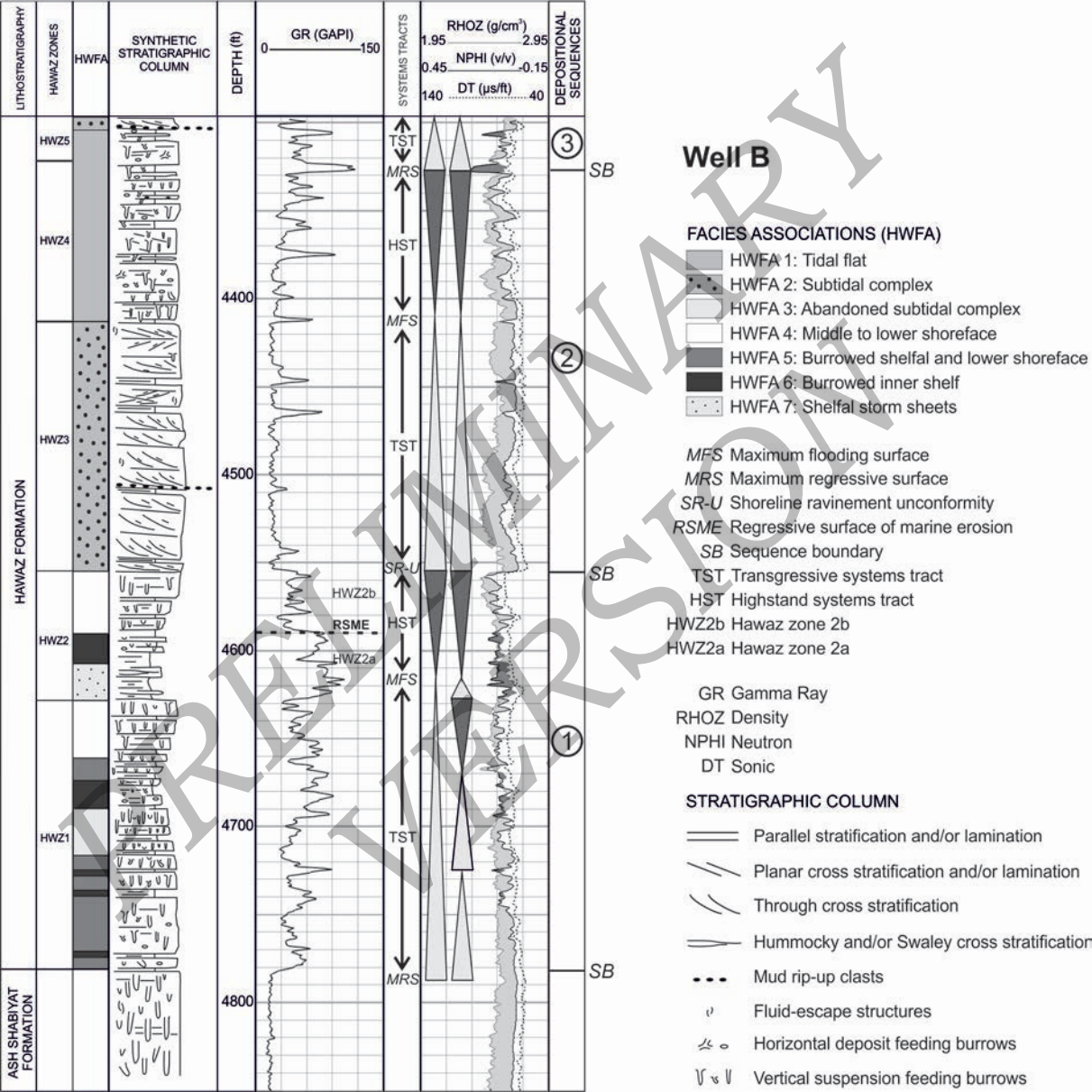
HWFA5
Burrowed shelfal and lower shoreface

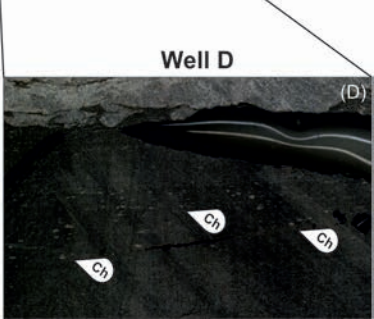
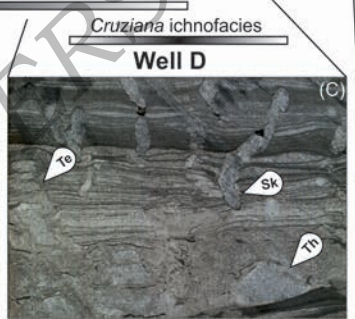
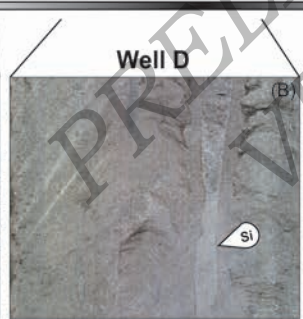
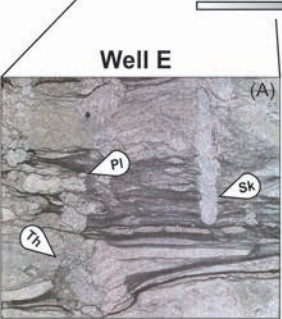
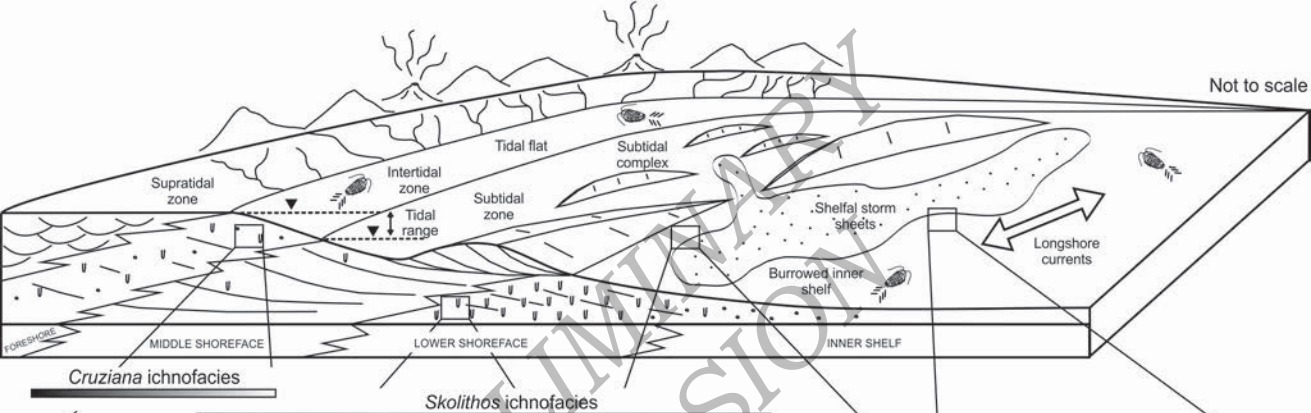
HWFA6
Burrowed inner shelf

HWFA7
Shelfal storm sheets









| | | |
|----------------|--------------------------|---|
| Sandstones (S) | Nonburrowed | <p>Sx1: Large-scale cross-bedded sandstones</p> <p>Sx2: Small- to medium-scale cross-bedded sandstones</p> <p>Sl: Parallel-laminated sandstones</p> <p>Sxl: Cross-laminated sandstones</p> <p>Sr: Ripple cross-laminated sandstones</p> <p>Sv: Massive sandstones</p> |
| | Burrowed (b) | <p>Sxb: Burrowed cross-bedded sandstones</p> <p>Sxlb: Burrowed cross-laminated sandstones</p> <p>Srb: Burrowed ripple cross-laminated sandstones</p> <p>Sb: Burrowed sandstones with Siphonichnus</p> <p>MSb: Burrowed sandstones with feeding ichnofauna</p> |
| | Sandy Heterolithics (HS) | <p>HS: Sandy heterolithics</p> <p>HSb: Burrowed sandy heterolithics</p> |
| | Muddy Heterolithics (HM) | <p>HM: Muddy heterolithics</p> <p>HMb: Burrowed muddy heterolithics</p> |

PRELIMINARY VERSION

| Processes / Controlling factors | Actualistic (Present) | Non-Actualistic (Early Paleozoic and older) |
|---------------------------------|--|--|
| Land flora | Vegetation in continental to transitional environments helps to stabilize river banks limiting channel shifting, changing river style from braided to meandering in low gradient systems | The lack of vegetation in subaerial conditions led to the development of high energy fluvial systems (mainly braided style) characterised by rapid channel shifting of rivers even in very low gradient systems |
| | Chemical weathering and related clay generation. | Lack of clay generation by induced chemical weathering due to the absence of vegetation in subaerial environments. Clay-size particles alternatively sourced from volcanic ash, hydrothermalism, diagenesis, etc. |
| Greenhouse / Icehouse | Incision of valleys during sea level fall in recent icehouse periods and subsequent development of estuarine environments with marine transgressions. Fluvial sediments are common in proximal parts of the systems and related hyperpycnal deposits in more distal settings during lowstand stages. | Epeiric seas in large cratonic basins during greenhouse periods developing areally extensive paralic environments. Very difficult to identify lowstand deposits due to very limited incision in proximal environments. Very low gradients imply major paleoshoreline shifts with only limited relative sea level rises |
| Tidal range | Lower tidal range caused by tidal energy dissipation due to larger distance between the Earth and the Moon with time. Maximum known current tidal range is about 12m (40ft) | Higher tidal range due to the reduced distance between the Earth and the Moon (unknown maximum tidal range in the early Paleozoic). |
| Ichnofacies | Broader and more diversified ichnofacies at present times. Characteristic <i>Skolithos</i> and <i>Cruziana</i> ichnofacies found in Hawaz Formation have different signature due to the presence of different fauna in present depositional environments. | Characteristic, often low diversity, mix of <i>Skolithos</i> and <i>Cruziana</i> ichnofacies is largely confined to the early Paleozoic, often occurring in the form of ichnofabrics characterised by a distinctive 'pipe rock' texture and trilobite traces. |